SONAR: Long-Range Graph Propagation Through Information Waves

Alessandro Trenta*
Department of Computer Science
University of Pisa
Pisa, Italy
alessandro.trenta@phd.unipi.it

Alessio Gravina*
Department of Computer Science
University of Pisa
Pisa, Italy
alessio.gravina@di.unipi.it

Davide Bacciu
Department of Computer Science
University of Pisa
Pisa, Italy
davide.bacciu@unipi.it

Abstract

Capturing effective long-range information propagation remains a fundamental yet challenging problem in graph representation learning. Motivated by this, we introduce SONAR, a novel GNN architecture inspired by the dynamics of wave propagation in continuous media. SONAR models information flow on graphs as oscillations governed by the wave equation, allowing it to maintain effective propagation dynamics over long distances. By integrating adaptive edge resistances and state-dependent external forces, our method balances conservative and non-conservative behaviors, improving the ability to learn more complex dynamics. We provide a rigorous theoretical analysis of SONAR's energy conservation and information propagation properties, demonstrating its capacity to address the long-range propagation problem. Extensive experiments on synthetic and real-world benchmarks confirm that SONAR achieves state-of-the-art performance, particularly on tasks requiring long-range information exchange.

1 Introduction

Graph neural networks (GNNs) [67, 76, 10, 18] have become a powerful framework for processing graph-structured data, enabling applications across various domains such as social networks [59, 49], molecular biology [36, 89, 43, 5], and more [38, 58]. Most GNNs are built upon the Message-Passing Neural Networks (MPNNs) framework [36], where information is exchanged between neighboring nodes, enabling effective learning from local graph structure. Despite their widespread use and success, a persistent challenge in GNNs is the effective modeling of long-range dependencies within graphs, as information propagation tends to degrade over extended distances. This is caused by phenomena such as over-smoothing [11, 73], over-squashing [2, 19], and, more generally, vanishing gradients [3]. Several recent approaches have been developed to better capture long-range dependencies in graphs, including graph rewiring [35, 83, 7], multi-hop GNNs [1, 46, 20], differential-equation-based GNNs (DE-GNNs) [13, 39, 40, 52], and graph transformers [78, 23, 90, 72, 88]. Graph transformers, in particular, have gained popularity due to their use of attention mechanisms, which allow any pair of nodes to exchange information directly. However,

*Equal contribution

39th Conference on Neural Information Processing Systems (NeurIPS 2025).

their quadratic computational cost poses scalability challenges. Moreover, recent studies have shown that, on some long-range tasks, they may actually perform worse than standard MPNNs [82].

To address the long-range propagation problem, we draw inspiration from wave propagation in continuous media, where signals can travel vast distances with minimal energy loss [29]. We propose **SONAR** (**S**tructured **O**scillatory Graph Neural **N**etwork with **A**daptive **R**esistance), a novel DE-GNN with a MPNN-like architecture that models information propagation through the lens of wave-based dynamics. Unlike diffusion-based propagation schemes such as [59, 85, 89], which are inherently dissipative and struggle to capture long-range interactions [3], wave-based dynamics preserve signal energy and enable effective communication across distant nodes. This mechanism is analogous to acoustic wave propagation in the ocean, where, under specific temperature and pressure gradients, sound waves can become trapped in the SOFAR channel [30]. This natural waveguide allows acoustic signals to travel across thousands of kilometers with minimal attenuation. SONAR adopts a similar principle in the graph domain: by treating information as a wave propagating through the graph topology, it maintains signal fidelity over many hops and facilitates robust long-range interactions. Specifically, it adopts a mathematically grounded formulation to model wave dynamics [34], resulting in inherently linear propagation dynamics with strong theoretical guarantees. Moreover, SONAR introduces adaptive resistances that enable each edge to control the flow of information, along with external forces that balance conservative and non-conservative dynamics, allowing the model to capture more complex behaviors and improve performance on downstream tasks.

The key contributions of this work are the following: (i) We propose SONAR, a novel MPNN-like architecture based on the wave equation for graphs, which enables the balance and integration of non-dissipative long-range propagation and non-conservative behaviors. Additionally, it incorporates adaptive resistances that allow each edge to modulate the information flow. (ii) We theoretically prove that, in its conservative form, SONAR does not dissipate the energy of features in the graph, i.e., information is preserved. In its continuous form, the sensitivity matrix between any two nodes never vanishes but oscillates following a cosine function. (iii) We employ additional dissipative and forcing terms, allowing SONAR to mediate between pure conservative and non-conservative behaviors. This gives SONAR the flexibility to learn to filter out irrelevant information. (iv) We conduct extensive experiments to demonstrate the benefits of our method. SONAR consistently achieves on par or better performance than existing methods across diverse tasks and benchmarks. Notably, SONAR outperforms existing state-of-the-art methods on synthetic long-range benchmarks, where accurate modeling of distant node interactions is crucial, highlighting its strength in long-range propagation.

2 Related Work

Long-Range Propagation in GNNs. Effectively modeling long-range dependencies remains a central challenge in deep learning for graphs [77, 3]. GNNs usually rely on local neighborhood aggregation, which limits their capacity to capture interactions between distant nodes [2, 19] due to challenges such as over-smoothing [11, 68, 73] and over-squashing [2, 83, 19], which are linked to the problem of vanishing gradients [3]. Therefore, GNNs based on message passing exhibit a performance degradation in tasks requiring more global context, such as molecular property prediction [24]. To address these challenges, a variety of strategies have been proposed. Graph rewiring methods, including SDRF [83], DIGL [35], FoSR [57], and DRew [46], modify the graph topology to facilitate long-range communication. Other approaches include regularizing the model's weight space [39, 41, 40], exploiting port-Hamiltonian dynamics [52], filtering messages in the information flow [28, 32], using a graph adaptive method based on a learnable ARMA framework [25], or using multi-hop information in a single update [21]. Graph Transformers [61, 72, 78, 80, 90] offer an alternative paradigm by enabling direct message passing between any pair of nodes via attention mechanisms. While effective, most of these methods often introduce additional computational complexity due to denser graph shift operators or all-pairs interactions.

GNNs based on Differential Equations. Recent advancements in the field of representation learning have introduced new architectures that establish a connection between neural networks and dynamical systems. Building on foundational work in recurrent neural networks [16, 47], this perspective has been extended to GNNs [50]. Indeed, works like GDE [71], GRAND [13], PDE-GCN [26], DGC [87], GRAND++ [81] propose to interpret GNNs as discretisations of ODEs and PDEs. Methods in this class impose a bias on node representation trajectories to follow the heat diffusion process [13, 81, 87], exploit non-dissipative dynamics [39, 40], or hamiltonian dynamics [56, 91, 52].GraphCON [74]

further explores oscillatory dynamics to preserve the Dirichlet energy encoded in the node features and mitigate oversmoothing. In GraphCON, each node acts as an oscillator that exchanges information with its neighbors through a simple GCN [59] or GAT [85]. In contrast, SONAR adopts a mathematically grounded formulation of graph calculus [33] to model wave propagation on graphs [34], resulting in inherently linear dynamics that offer stronger theoretical guarantees for long-range information propagation. Moreover, SONAR introduces adaptive resistances (which allow each edge to modulate how information is transmitted) as well as external forces that enable the modeling of more complex dynamics. The spatio-temporal evolution of graphs has been studied in [27, 42, 55, 44].

3 SONAR

In this section, we introduce our **SONAR** (**S**tructured **O**scillatory Graph Neural **N**etwork with **A**daptive **R**esistance), a novel GNN architecture whose information flow is designed as the wave equation on graphs, enabling long-range information propagation between nodes. Figure 1 provides a visual representation of the overall architecture and wave propagation dynamics.

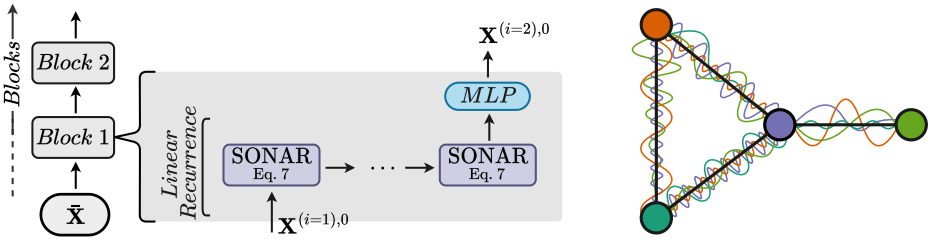

(a) Deep SONAR architecture

(b) SONAR propagation dynamics

Figure 1: Illustration of (a) a deep SONAR architecture and (b) the SONAR propagation dynamics of one block.

3.1 Notations and Preliminaries

We consider a graph $\mathcal{G} = (\mathcal{V}, \mathcal{E})$ as the system of interacting entities called nodes, where $\mathcal{V}$ is a set of n nodes and $\mathcal{E} \subseteq \mathcal{V} \times \mathcal{V}$ is a set of m edges. The structural information expressed by $\mathcal{E}$ can be encoded in the adjacency matrix $\mathbf{A} \in \{0,1\}^{n \times n}$, i.e., a binary matrix where $\mathbf{A}_{ij} = 1$ if $(i,j) \in \mathcal{E}$ and zero otherwise. We define the neighborhood of node v as the set of nodes u directly linked with v, i.e., $\mathcal{N}(v) = \{u | \mathbf{A}_{uv} = 1\}$, and the degree of node v as the number of its neighbors, $\deg(v) = |\mathcal{N}(v)|$. Lastly, we consider the Laplacian matrix $\mathbf{L}$ and two normalizations, i.e., symmetric and random-walk normalized Laplacian matrices, which are respectively defined as

$$\mathbf{L} = \mathbf{D} - \mathbf{A}, \qquad \mathbf{L}^{\text{sym}} = \mathbf{I} - (\mathbf{D}^{+})^{\frac{1}{2}} \mathbf{A} (\mathbf{D}^{+})^{\frac{1}{2}}, \qquad \mathbf{L}^{\text{rw}} = \mathbf{I} - \mathbf{D}^{+} \mathbf{A} \tag{1}$$

where $\mathbf{I}$ is the identity matrix, $\mathbf{D}$ is the diagonal degree matrix with $\mathbf{D}_{ii} = \deg(v_i)$ and v_i a generic node. $\mathbf{D}^{+}$ is the pseudo-inverse of $\mathbf{D}$. Following [34], the definition of graph Laplacian can be generalized to its weighted version and to any node function $f(v) : \mathcal{V} \to \mathbb{R}$ as

$$(\Delta f)(v) = (\mathbf{L}^{a} f)(v) = (\mathbf{D}^{a} f)(v) - (\mathbf{A}^{a} f)(v) = \sum_{u \in \mathcal{N}(v)} a_{uv} (f(v) - f(u)) \tag{2}$$

where $\mathbf{D}^{a}$ and $\mathbf{A}^{a}$ are the weighted degree and adjacency matrices, and $a_{uv} \in \mathbb{R}_{+}$ is a weight on the directed edge $(u,v) \in \mathcal{E}$.

Each node in the graph is associated with a hidden state vector $\mathbf{x}_v(t) \in \mathbb{R}^d$, which provides the evolution of the node representation at time t in the system. The term $\mathbf{X}(t) = [\mathbf{x}_0(t), \ldots, \mathbf{x}_{n-1}(t)]^{\top} \in \mathbb{R}^{n \times d}$ is the matrix of all node states at time t. We note that in the domain of differential-equations the continuous dynamics expressed by the neural network is discretized into classical GNN layers [39]. Therefore, given the initial condition (node input features) $\mathbf{x}_v(0) = \bar{\mathbf{x}}_v$, each GNN layer $\ell = 1, \ldots, L$ computes node states $\mathbf{x}_v^{\ell}$ which approximate $\mathbf{x}_v(t = h\ell)$, with h being the integration step size.

The wave equation in physics. Waves in physics describe the propagation of oscillations in a continuous medium. Common examples are electromagnetic waves [62] and sound waves [48]. These are described by the wave equation $\frac{\partial^2 f}{\partial t^2} = c^2 \frac{\partial^2 f}{\partial x^2}$, where $f(t, x)$ is a scalar function describing the wave and c is its propagation speed, which is an intrinsic characteristic of the conditions and medium. Directly descending from their equation, waves have interesting properties: (i) they can travel indefinitely without losing amplitude and energy at constant speed [29], and (ii) they can be linearly composed and decomposed, allowing for superposition of waves propagating from different directions [62]. More specifically, the total energy $E(t)$ of a wave on $\mathbb{R}$ is defined as

$$E(t) = \int_{\mathbb{R}} \left(\frac{\partial f}{\partial t}\right)^2 + \left(\frac{\partial f}{\partial x}\right)^2 dx, \tag{3}$$

and can be shown to be constant [29] in the whole space and even on bounded domains. Our objective is to exploit these properties to propagate energy and information indefinitely a graph.

Waves following a non-conservative dynamic can be modeled with the addition of a dissipative term $D(t, x) = k\frac{\partial f}{\partial t}(t, x)$, which dampens the wave and dissipates energy, or with an external forcing term $F(t, x)$, which represents other environmental factors acting on the wave.

3.2 The SONAR wave propagation

To model information propagation on graphs as oscillations in a continuous medium, we formulate the dynamics of SONAR through a differential equation that follows the graph wave equation. Specifically, we start by defining the evolution of node states as:

$$\ddot{\mathbf{X}}(t) = -\mathbf{L}\mathbf{X}(t)\mathbf{W}, \qquad \mathbf{X}(0) = \bar{\mathbf{X}}, \tag{4}$$

where $\ddot{\mathbf{X}}(t)$ is the second-order derivative of $\mathbf{X}(t)$, $\mathbf{W} \in \mathbb{R}^{d\times d}$ is a learnable weight matrix, and $\bar{\mathbf{X}}$ contains the initial node states. To more closely mimic wave propagation in physical media, we adopt the weighted graph Laplacian in Equation (2), allowing different edges to modulate how signals travel through the graph. In other words, each pairwise communication between nodes can be viewed as residing in a distinct medium, where the wave properties, e.g., speed and amplitude, vary depending on the properties of the medium. This is analogous to propagating signals at different depths in the ocean, where specific water temperature and pressure alter the wave propagation capabilities. Therefore, in our setting, the Laplacian weight a_{uv} can be interpreted as an inverse resistance term that governs the ease with which information flows between nodes u and v. Although a_{uv} can be implemented as static (fixed) weights, in our experiments in Section 4 we employ neural networks to learn such weights in order to adaptively model the dynamics of the propagation on the specific task.[2]

To further cast the system dynamics in the more general setting, we then introduce the possibility of trading between the conservative behaviour typical of undampened wave equations (discussed in detail in Section 3.3) with non-conservative dynamics. We introduce dissipative and external forcing terms to alter the conservative evolution of node states. Therefore, Equation (4) can be rewritten to include the new terms as

$$\ddot{\mathbf{X}}(t) = -\mathbf{L}^a\mathbf{X}(t)\mathbf{W} - D(\mathbf{X}(t)) \odot \dot{\mathbf{X}}(t) + F(\mathbf{X}(t)), \tag{5}$$

where $D(\mathbf{X}(t)) \in \mathbb{R}_+^{n\times d}$ and $F(\mathbf{X}(t)) \in \mathbb{R}^{n\times d}$ denote the state-dependent dissipative and external forcing terms, respectively. $\odot$ is the Kronecker product. We note that without $D(\mathbf{X}(t))$ and $F(\mathbf{X}(t))$, the purely conservative inductive bias of the wave equations constrains node states to evolve along conservative trajectories, which may limit the model's effectiveness and hinder its ability to capture the more complex dynamics required for downstream tasks. Therefore, the dissipative term allows irrelevant information to be dissipated during propagation, while the external force introduces additional flexibility to control the dynamics based on input-dependent signals. In our experiments in Section 4, we employ neural networks to learn both the dissipative and external forcing terms.

Discretization and implementation details. As for standard DE-GNNs, a numerical discretization method is needed to solve Equation (5). We solve the equation with a finite difference scheme [31].

[2]Note that disconnected nodes always have a zero adaptive resistance. Thus, the resistance a_{uv} is calculated only between connected nodes.

To this aim, we first introduce the auxiliary velocity variable to be the first-order derivative of the node states, i.e., $\mathbf{V}(t) = \dot{\mathbf{X}}(t)$, to rewrite Equation (5) as the first-order system:

$$\begin{cases} \dot{\mathbf{X}}(t) = \mathbf{V}(t) \\ \dot{\mathbf{V}}(t) = -\mathbf{L}^a \mathbf{X}(t)\mathbf{W} - D(\mathbf{X}(t)) \odot \dot{\mathbf{V}}(t) + F(\mathbf{X}(t)). \end{cases} \tag{6}$$

This system can be now discretized by iteratively solving

$$\begin{cases} \mathbf{X}^{\ell+1} = \mathbf{X}^{\ell} + h\mathbf{V}^{\ell+1}, \\ \mathbf{V}^{\ell+1} = \mathbf{V}^{\ell} - h\left(\mathbf{L}^a \mathbf{X}^{\ell}\mathbf{W} + D(\mathbf{X}^{\ell}) \odot \mathbf{V}^{\ell} - F(\mathbf{X}^{\ell})\right), \end{cases} \tag{7}$$

where h is the step size of the discretization method, and $\mathbf{X}^0 = \bar{\mathbf{X}}$ and $\mathbf{V}^0 = \mathbf{X}^0\mathbf{W}_V$, with $\mathbf{W}_V \in \mathbb{R}^{d\times d}$ a learnable matrix for the initial velocity. Note that edge features can be seamlessly incorporated into Equation (7), as detailed in Appendix A.1. As discussed above, we can discretize time into GNN layers, such that the embedding $\mathbf{x}_v^{\ell}$ from Equation (7) encodes information that is ℓ hops away from v.

We note that, when dissipation and external forcing are not employed, information is linearly aggregated. To increase effectiveness, we can build a deep architecture for our SONAR, following principles established in modern architectures [69, 45, 12]. Therefore, we define a SONAR block by applying an MLP to the output of Equation (7) after L propagation steps, introducing nonlinear dynamics into the model. Multiple SONAR blocks can then be stacked to form a deep architecture, where the output of block i becomes the initial condition of the subsequent block $(i+1)$:

$$\begin{aligned} \mathbf{X}^{(i),L} &= \text{SONAR}(\mathbf{X}^{(i),0}) \\ \mathbf{X}^{(i+1),0} &= \text{MLP}(\mathbf{X}^{(i),L}). \end{aligned} \tag{8}$$

This concept is visually summarized in Figure 1a.

In our experiments in Section 4, the Laplacian weights a_{uv} are implemented as the output of an MLP that takes the states $\mathbf{x}_v^{\ell}$ and $\mathbf{x}_u^{\ell}$ as input, followed by a ReLU activation to ensure a positive output. The dissipative term is modeled using an MLP applied to the current node state, also followed by a ReLU to enforce non-negative outputs. The external forcing term is computed via an MLP without activation constraints, allowing it to output both positive and negative values. As a result, each propagation step (i.e., iteration of the discretization step) ℓ in each block is associated with its own set of learned Laplacian weights, as well as dissipative and external forces. Each SONAR block is equipped with its own set of parameters for learning the Laplacian weights, the dissipative and external forcing components, as well as its own learnable matrices for initial velocity $\mathbf{W}_V^{(i)}$, and message passing aggregation weights $\mathbf{W}^{(i)}$ (which are shared within the block). We consider both the number of blocks and propagation steps as hyperparameters in our experiments.

3.3 Theoretical Properties of SONAR

We now provide theoretical statements about energy and information conservation properties of SONAR, showing that our model effectively performs long-range propagation between nodes. Appendix B provides the proofs for the statements.

SONAR allows for long-range propagation. To prove that SONAR has a conservative behavior, we start by defining the energy of the system, adapting Equation (3) to the graph domain, as

$$E(t) = \underbrace{\sum_{v\in V} \frac{1}{2}\|\nabla \mathbf{x}_v(t)\|^2}_{\text{potential energy}} + \underbrace{\frac{1}{2}\left\|\frac{\partial \mathbf{X}(t)}{\partial t}\right\|^2}_{\text{kinetic energy}}. \tag{9}$$

The energy contains two components: the potential energy, which measures how much the signal varies across the graph (i.e., spatial variation)[3]; and the kinetic energy, which captures how node states change over time (i.e., layer-wise variation). In other words, the kinetic energy tells how fast the wave is vibrating, while the potential energy reflects the tension in the system. By maintaining a constant energy, we therefore ensure that node information is preserved during propagation.

[3]The potential energy is equivalent with the Dirichlet energy in [37] employed to measure over-smoothing.

To better highlight how node coupling and SONAR convolution affect energy conservation in the graph, we now focus on a single feature $\mathbf{X}(t) \in \mathbb{R}^n$. The generalization to multiple features is left to Appendix B. The following theorem shows that without dissipation and external forcing (i.e., with a propagation similar to Equation (4)), the wave propagation through the graph conserves the energy.

Theorem 3.1. *Let $\mathbf{X}(t) \in \mathbb{R}^n$ be the node states at time t, obtained as the solution to the graph wave equation in Equation* (5)*, with initial condition $\mathbf{X}(0) = \bar{\mathbf{X}}$, null dissipative and external forcing terms. Then, the energy $E(t)$ in Equation* (9) *is conserved, that is, $E(t) = E(0)\ \forall t > 0$.*

This result implies that information encoded in the node states is neither amplified nor dissipated over time (i.e., while traversing the graph), but redistributed in a lossless manner across the graph. This property enables SONAR to perform deeper propagation, making it particularly suitable for tasks requiring long-range interactions.

To provide a clearer picture of the long-range capabilities of our SONAR, we follow the recent literature [83, 19] and evaluate the long-range propagation ability by measuring the sensitivity of the node states. Specifically, we first measure how sensitive is a node state at an arbitrary time t with respect to the initial state of another node, i.e., $\partial \mathbf{x}_v(t)/\partial \mathbf{x}_u(0)$. Then, we compute the same sensitivity for the discretization version of our SONAR, i.e., $\partial \mathbf{x}_v^\ell / \partial \mathbf{x}_u^0$, and compute its norm similarly to [19]. We consider SONAR with null dissipative and external forcing terms, and initial conditions $\mathbf{X}(0) = \bar{\mathbf{X}} \in \mathbb{R}^n, \mathbf{V}(0) = \mathbf{0}$. The explicit solution of our system (following [34]) is

$$\mathbf{X}(t) = \cos\left(t\sqrt{\mathbf{L}}\right)\bar{\mathbf{X}}, \tag{10}$$

where $\cos\left(t\sqrt{\mathbf{L}}\right) = \sum_{n=0}^{\infty}(-1)^n \frac{t^{2n}}{n!}\sqrt{\mathbf{L}}^{2n}$. We drop the Laplacian superscript ^{a} to ease notation and explicitly write the sensitivity matrix in the following theorem.

Theorem 3.2 (Sensitivity matrix, continuous case)**.** *Let $\mathbf{x}_v(t)$ be the state for node v at time t. Then, the sensitivity $\frac{\partial \mathbf{x}_v(t)}{\partial \mathbf{x}_u(0)}$ between nodes u and v is*

$$\frac{\partial \mathbf{x}_v(t)}{\partial \mathbf{x}_u(0)} = \cos\left(t\sqrt{\mathbf{L}}\right)_{vu}. \tag{11}$$

The proof is a consequence of the solution in Equation (10). Theorem 3.2 shows that the influence of node u on node v oscillates following a cosine function, but never vanishes definitively.

We now consider a full discrete message passing with state vectors $\mathbf{X}^\ell \in \mathbb{R}^{n\times d}$ and measure the sensitivity after ℓ steps (i.e., layers).

Theorem 3.3 (One-step sensitivity matrix, discrete case)**.** *The sensitivity matrix $\frac{\partial \mathbf{x}_v^\ell}{\partial \mathbf{x}_u^{\ell-1}} \in \mathbb{R}^{d\times d}$ of Equation* (7) *with null dissipative and external forcing terms is given by*

$$\frac{\partial \mathbf{x}_v^\ell}{\partial \mathbf{x}_u^{\ell-1}} = 2\mathbf{I}_{uv} - h^2 \mathbf{L}_{uv}\mathbf{W}. \tag{12}$$

The step size h balances two components: the residual information from the node itself, related to the term $2\mathbf{I}_{uv}$, and the signal coming from neighboring nodes, related to $\mathbf{L}_{uv}\mathbf{W}$. This last term is also proportional to the difference between node features (see the definition of the graph Laplacian in Equation 2), encouraging the exchange of information when neighboring nodes are different.

Similarly to [19], we now assess sensitivity of our SONAR in Equation (7) for the full non-conservative case, i.e., with dissipation and external forcing.

Theorem 3.4 (Sensitivity bound, discrete case)**.** *Consider the SONAR in Equation* (7) *on node states $\mathbf{X}(t) \in \mathbb{R}^{n\times d}$. Let the dissipation coefficient be such that $|D(\mathbf{X}^\ell)| \le k$ and the external forcing be $F(\mathbf{X}^\ell) = \mathbf{X}^\ell \mathbf{W}_F$. Let the initial velocity be calculated as $\mathbf{V}(0) = \bar{\mathbf{X}}\mathbf{W}_V$. Finally, let $w = \max\{|\mathbf{W}|, |\mathbf{W}_F|, |\mathbf{W}_V|, 1\}$. Then, the sensitivity matrix has the following upper bound*

$$\left\| \frac{\partial \mathbf{x}_v^\ell}{\partial \mathbf{x}_u^0} \right\|_{L_1} \le (wd)^\ell \left(\left((1 + h + h^2(N + k + 1))\mathbf{I} + h^2\mathbf{A}\right)^\ell \right)_{vu} \tag{13}$$

where $N = \max_{v\in V} N_v = \max_{v\in V} |\mathcal{N}(v)|$ is the maximum degree in the graph, d is the number of node features, and h is the step size of the discretization.

This result demonstrates that the sensitivity of SONAR remains well-controlled across layers. We note that classical MPNNs usually include a factor c_σ^ℓ in the bound, with c_σ the Lipschitz constant of the nonlinearity σ. In practice, this term often decay extremely fast, limiting the ability of standard MPNNs to propagate information over long distances. By contrast, the linear propagation dynamics of our SONAR allows for stable long-range information flow. Therefore, together with the previous theoretical results, it holds the capability of SONAR to perform long-range propagation effectively.

We remark that Theorem 3.1 and Theorem 3.2 do not depend on the choice of the discretization of the solution, while the results in Theorem 3.3 and Theorem 3.4, which explicitly depend on the step size, can be easily extended to any other integration procedure.

Complexity Analysis. SONAR consists of a stack of blocks, each with complexity of an MPNN (e.g., [59, 89]). Specifically, each iteration of Equation (7) is linear in the number of nodes (n) and edges (m), therefore it has a complexity of $\mathcal{O}(n+m)$. Assuming that L iterations are performed, a SONAR block has a complexity of $\mathcal{O}(L(n+m)+\rho)$, where ρ is the complexity of the MLP at the end of the block, as defined in Equation (8).

4 Experiments

In this section, we empirically validate the practical benefits of our method on popular graph benchmarks for long-range propagation as well as heterophilic node classification tasks. In Sections 4.1 and 4.2, we assess SONAR on synthetic benchmarks that require the exchange of messages between far-away nodes, thus performing long-range propagation. Specifically, we consider the graph transfer tasks from [40] and the task of predicting three graph properties from [39]. With the same purpose, we verify our method on the real-world long-range graph benchmark [24] in Section 4.3. Moreover, we assess the performance of SONAR on heterophilic tasks from [70] in Section 4.4. In Section 4.5, we empirically assess the long-range capabilites of SONAR in terms of the sensitivity metric (discussed in Section 3.3). In Appendix C.2, we report additional ablation studies to provide a more comprehensive understanding of SONAR, discussing runtimes and the role of adaptive resistance, dissipation, external forces, and step size. The performance of SONAR is compared with state-of-the-art methods, such as MPNNs, DE-GNNs, higher-order GNNs, and graph transformers, detailing the employed baselines in Appendix A.2. We report the hyperparameter space used in our experiments in Appendix A.4. All the experiments are performed on a server with NVIDIA H100 GPUs. We openly release the code at `https://github.com/gravins/SONAR`.

4.1 Graph Transfer Task

Setup. We consider the graph transfer task proposed by [19] under the experimental setting of [40]. The objective of this experiment is to transfer a label from a source to a target node placed at increasing distance ℓ, and measure how much information is propagated through the graph. We initialize nodes with a random valued feature, and we assign values "1" and "0" to source and target nodes, respectively. We consider three graph distributions, i.e., line, ring, crossed-ring, and four different distances $\ell = \{3, 5, 10, 50\}$. Thus, we consider short to extreme long-range scenarios. As ℓ increases, the task becomes progressively more challenging, demanding more effective long-range information propagation. Due to oversquashing, the performance is expected to deteriorate with larger ℓ. Consequently, addressing this problem requires methods with increasingly robust mechanisms for maintaining information flow across distant nodes. For this experiment, we use the same data, hyperparameter space, and experimental setting of [40].

Results. The results of SONAR and baseline models on the graph transfer task are shown in Figure 2, where we report the test mean squared error with standard error bars as a function of the distance between the source and target nodes. This task is specifically designed to evaluate a model's ability to propagate information across varying distances, making it a critical benchmark for assessing long-range capabilities. SONAR clearly outperforms all baselines at large distances (most notably at 50 hops) empirically validating its ability to support long-range information propagation. Moreover, SONAR achieves state-of-the-art performance across all tested distances, including shorter settings such as 3, 5, and 10 hops. Notably, while other models exhibit significant degradation as the distance increases, SONAR maintains a nearly constant error, demonstrating that it can propagate information effectively over both short and long ranges with consistent accuracy.

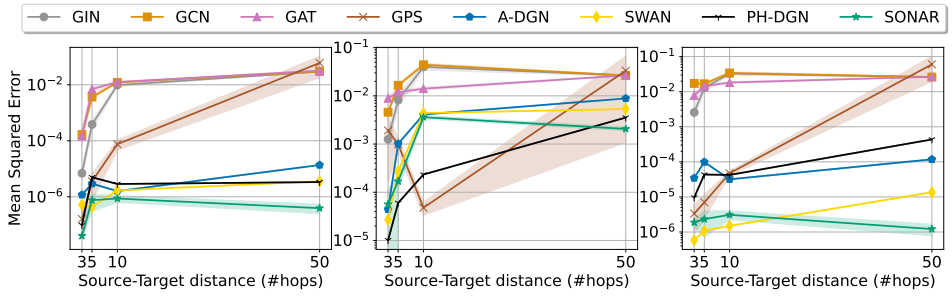

(a) Line (b) Ring (c) Crossed-Ring

Figure 2: Information transfer performance on (a) Line, (b) Ring, and (c) Crossed-Ring graphs. Overall, SONAR transfers the information more accurately as distance increases, achieving a lower error than non-dissipative methods (i.e., A-DGN, SWAN, PH-DGN) and transformers (i.e., GPS).

4.2 Graph Property Prediction

Setup. We consider the three graph property prediction tasks proposed in [39] and investigate the performance of our SONAR in predicting graph diameter, single source shortest path (SSSP), and node eccentricity on synthetic graphs sampled from multiple distributions. These tasks inherently demand the ability to capture and transmit information across the graph, as they are based on shortest-path computations. Indeed, similarly to standard algorithmic approaches (e.g., Bellman-Ford, Dijkstra's algorithm), accurate solutions depend on the exchange of multiple messages between nodes. Consequently, models that struggle with long-range propagation result in poor performance. For this experiment, we use the same data, hyperparameters space, and experimental setting presented in [39].

Table 1: Mean test set $log_{10}(\text{MSE})(\downarrow)$ and std averaged on 4 random weight initializations on Graph Property Prediction tasks. The lower, the better. **First**, **second**, and **third** best results for each task are color-coded.

Model	Diameter	SSSP	Eccentricity
MPNNs			
GCN	0.7424$_{\pm 0.0466}$	0.9499$_{\pm 0.0001}$	0.8468$_{\pm 0.0028}$
GAT	0.8221$_{\pm 0.0752}$	0.6951$_{\pm 0.1499}$	0.7909$_{\pm 0.0222}$
GraphSAGE	0.8645$_{\pm 0.0401}$	0.2863$_{\pm 0.1843}$	0.7863$_{\pm 0.0207}$
GIN	0.6131$_{\pm 0.0990}$	-0.5408$_{\pm 0.4193}$	0.9504$_{\pm 0.0007}$
GCNII	0.5287$_{\pm 0.0570}$	-1.1329$_{\pm 0.0135}$	0.7640$_{\pm 0.0355}$
AMP	-0.5891$_{\pm 0.0720}$	-3.9579$_{\pm 0.0769}$	0.0515$_{\pm 0.1819}$
DE-GNNs			
DGC	0.6028$_{\pm 0.0050}$	-0.1483$_{\pm 0.0231}$	0.8261$_{\pm 0.0032}$
GRAND	0.6715$_{\pm 0.0490}$	-0.0942$_{\pm 0.3897}$	0.6602$_{\pm 0.1393}$
GraphCON	0.0964$_{\pm 0.0620}$	-1.3836$_{\pm 0.0092}$	0.6833$_{\pm 0.0074}$
A-DGN	-0.5188$_{\pm 0.1812}$	-3.2417$_{\pm 0.0751}$	0.4296$_{\pm 0.1003}$
SWAN	-0.5981$_{\pm 0.1145}$	-3.5425$_{\pm 0.0830}$	-0.0739$_{\pm 0.2190}$
PH-DGN	-0.5473$_{\pm 0.1074}$	**-4.2993**$_{\pm 0.0721}$	-0.9348$_{\pm 0.2097}$
Graph Transformers			
GPS	-0.5121$_{\pm 0.0426}$	**-3.5990**$_{\pm 0.1949}$	0.6077$_{\pm 0.0282}$
Multi-hop GNNs			
DRew-GCN	**-2.3692**$_{\pm 0.1054}$	-1.5905$_{\pm 0.0034}$	**-2.1004**$_{\pm 0.0256}$
+ delay	**-2.4018**$_{\pm 0.1097}$	-1.6023$_{\pm 0.0078}$	**-2.0291**$_{\pm 0.0240}$
Our			
SONAR	**-3.2906**$_{\pm 0.0706}$	**-6.7517**$_{\pm 0.0590}$	**-3.1187**$_{\pm 0.0192}$

Results. We report results using the $log_{10}(\text{MSE})$ metric in Table 1. This benchmark focuses on predicting shortest-path-based properties that inherently require the model to capture the global graph structure, thus long-range information. SONAR sets a new performance standard by outperforming all existing methods by at least one order of magnitude across all tasks. While standard MPNNs struggle to model such properties due to their limited ability to propagate information over long distances, SONAR consistently surpasses DE-GNNs (its direct competitors), multi-hop GNNs, and transformer-based models, which are typically more computationally demanding. Notably, SONAR improves over the best-performing baseline by 0.89 points on Diam., 1.01 on Ecc., and a remarkable 2.46 on the SSSP task, further demonstrating its effectiveness in capturing long-range dependencies.

4.3 Long-Range Graph Benchmark

Setup. To assess the performance on real-world long-range benchmarks, we consider the "Peptides-func", "Peptides-struct", "PascalVOC-SP" tasks [24]. The first two tasks involve predicting the functional or structural properties of graphs derived from peptides, which are large molecules based on amino acid chains. Similarly to previous tasks, accurate predictions require effectively capturing long-range interactions, as these properties are determined by the interplay between distant regions of the graphs, i.e., peptides. The "PascalVOC-SP" is a node-classification task on superpixel

graphs, which is considered to be more difficult than the peptides ones in the long-range context [6]. We use the same data and experimental setting in [24], including the 500k parameter budget.

Results. We present the performance of SONAR alongside leading baselines in Table 2, with a more extended comparison in Appendix C.1. SONAR achieves significantly better results than standard MPNNs and generally outperforms most DE-GNNs (i.e., SONAR's model class) and multi-hop GNNs across all tasks. On `func`, SONAR ranks second overall, only one point behind DRew, which relies on expensive graph rewiring. On `struct`, SONAR achieves a performance with standard deviation overlapping with top models. On `PascalVOC-SP`, SONAR improves the F1 score of transformer models by a remarkable 8.3%, ranking first with or without positional encoding. Overall, compared to transformer-based models with quadratic complexity, SONAR achieves comparable or better performance while maintaining linear complexity. We conclude that the long-range capabilities of SONAR are also evident in real-world tasks.

Table 2: Results for Peptides-func, Peptides-struct and PascalVOC-SP averaged over 3 training seeds. Baseline results are taken from [24, 46, 51, 65, 40, 52]. Note that all MPNN-based methods include structural and positional encoding. The **first**, **second**, and **third** best scores are colored.

Model	Peptides-func AP ↑	Peptides-struct MAE ↓	Pascal VOC-SP F1 ↑
MPNNs			
GatedGCN	$58.64_{\pm 0.77}$	$0.3420_{\pm 0.0013}$	$0.2873_{\pm 0.0219}$
GCN	$59.30_{\pm 0.23}$	$0.3496_{\pm 0.0013}$	$0.1268_{\pm 0.0060}$
GCNII	$55.43_{\pm 0.78}$	$0.3471_{\pm 0.0010}$	$0.1698_{\pm 0.0080}$
GINE	$54.98_{\pm 0.79}$	$0.3547_{\pm 0.0045}$	$0.1265_{\pm 0.0076}$
Multi-hop GNNs			
DIGL+MPNN+LapPE	$68.30_{\pm 0.26}$	$0.2616_{\pm 0.0018}$	$0.2921_{\pm 0.0038}$
DRew-GCN	$69.96_{\pm 0.76}$	$0.2781_{\pm 0.0028}$	$0.1848_{\pm 0.0107}$
DRew-GCN+LapPE	**71.50**$_{\pm 0.44}$	$0.2536_{\pm 0.0015}$	$0.1851_{\pm 0.0092}$
MixHop-GCN	$65.92_{\pm 0.36}$	$0.2921_{\pm 0.0023}$	$0.2506_{\pm 0.0133}$
MixHop-GCN+LapPE	$68.43_{\pm 0.49}$	$0.2614_{\pm 0.0023}$	$0.2218_{\pm 0.0174}$
Transformers			
GraphGPS+LapPE	$65.35_{\pm 0.41}$	$0.2500_{\pm 0.0005}$	**0.3748**$_{\pm 0.0109}$
Graph ViT	$69.42_{\pm 0.75}$	**0.2449**$_{\pm 0.0016}$	–
GRIT	$69.88_{\pm 0.82}$	**0.2460**$_{\pm 0.0012}$	–
SAN+LapPE	$63.84_{\pm 1.21}$	$0.2683_{\pm 0.0043}$	$0.3230_{\pm 0.0039}$
Transformer+LapPE	$63.26_{\pm 1.26}$	$0.2529_{\pm 0.0016}$	$0.2694_{\pm 0.0098}$
DE-GNNs			
GRAND	$57.89_{\pm 0.62}$	$0.3418_{\pm 0.0015}$	$0.1918_{\pm 0.0097}$
GraphCON	$60.22_{\pm 0.68}$	$0.2778_{\pm 0.0018}$	$0.2108_{\pm 0.0091}$
A-DGN	$59.75_{\pm 0.44}$	$0.2874_{\pm 0.0021}$	$0.2349_{\pm 0.0054}$
SWAN	$67.51_{\pm 0.39}$	$0.2485_{\pm 0.0009}$	$0.3192_{\pm 0.0250}$
PH-DGN	**70.12**$_{\pm 0.45}$	**0.2465**$_{\pm 0.0020}$	–
Ours			
SONAR	$68.42_{\pm 0.11}$	$0.2525_{\pm 0.0038}$	**0.4058**$_{\pm 0.0039}$
SONAR+LapPE	**70.47**$_{\pm 0.41}$	$0.2486_{\pm 0.0006}$	**0.4082**$_{\pm 0.0037}$

4.4 Heterophilic Tasks

Setup. To further evaluate the performance of our SONAR, we assess its the effectiveness in capturing complex relational information in heterophilic settings, where nodes belonging to same class are often connected through longer and sparser paths, we consider the five node classification tasks introduced in [70]. Specifically, we consider the "Roman-empire", "Amazon-ratings", "Minesweeper", "Tolokers", and "Questions" datasets. We adhere to the same data and experimental setting presented in [70].

Results. We report the results in Table 3 (extended comparison in Appendix C.1). SONAR achieves the best performance on both the `Roman-empire` and `Minesweeper` tasks, surpassing the second-best models by 0.8 and 2.8 points, respectively. It also performs competitively on `Amazon-ratings` and `Tolokers`, with less than one point difference from the top models and overlapping stds. Remarkably, SONAR outperforms all heterophily-designated GNNs by up to 20 points, except for the `Questions` dataset. This shows the flexibility of our approach on different tasks.

4.5 Empirical Sensitivity Analysis

We empirically assess the long-range capabilities of SONAR compared to a standard GCN, which can be considered as the most comparable baseline to our proposed SONAR. Both rely on the Laplacian operator and message-passing paradigm, but GCN lacks energy preservation guarantees for long-range information propagation, adaptive resistance, and external forces. For this analysis, we consider the Line task in Section 4.1 with $\ell = 50$ and measure the norm of the sensitivity matrix in Equation (13) between any node v and the source node u. Specifically, we compute the sensitivity considering increasing distance between u and v (i.e., 10, 20, 30, 40, 50) with respect to increasing values of model recurrences (i.e., number of explored hops). The results, reported in Table 4, confirm our theoretical findings in Section 3.3: the information propagation of SONAR leads to sensitivity norms that never vanish, even at higher distances. On the contrary, the dissipative dynamics of the GCN cause an exponential decay in the influence from the source node to distant nodes.

Table 3: Mean test set score and std averaged over 4 random weight initializations on heterophilic datasets. The higher, the better. **First**, **second**, and **third** best results for each task are color-coded.

Model	Roman-empire Acc ↑	Amazon-ratings Acc ↑	Minesweeper AUC ↑	Tolokers AUC ↑	Questions AUC ↑
MPNNs					
GAT	80.87±0.30	49.09±0.63	92.01±0.68	83.70±0.47	77.43±1.20
Gated-GCN	74.46±0.54	43.00±0.32	87.54±1.22	77.31±1.14	76.61±1.13
GCN	73.69±0.74	48.70±0.63	89.75±0.52	83.64±0.67	76.09±1.27
SAGE	85.74±0.67	**53.63**±0.39	**93.51**±0.57	82.43±0.44	76.44±0.62
Graph Transformers					
Exphormer	**89.03**±0.37	**53.51**±0.46	90.74±0.53	**83.77**±0.78	73.94±1.06
NAGphormer	74.34±0.77	51.26±0.72	84.19±0.66	78.32±0.95	68.17±1.53
GOAT	71.59±1.25	44.61±0.50	81.09±1.02	83.11±1.04	75.76±1.66
GPS	82.00±0.61	**53.10**±0.42	90.63±0.67	**83.71**±0.48	71.73±1.47
$\text{GPS}_{\text{GAT+Performer}}$ (RWSE)	87.04±0.58	49.92±0.68	91.08±0.58	**84.38**±0.91	77.14±1.49
GT	86.51±0.73	51.17±0.66	91.85±0.76	83.23±0.64	**77.95**±0.68
GT-sep	**87.32**±0.39	52.18±0.80	**92.29**±0.47	82.52±0.92	**78.05**±0.93
Heterophily-Designated GNNs					
FAGCN	65.22±0.56	44.12±0.30	88.17±0.73	77.75±1.05	77.24±1.26
FSGNN	79.92±0.56	52.74±0.83	90.08±0.70	82.76±0.61	**78.86**±0.92
GBK-GNN	74.57±0.47	45.98±0.71	90.85±0.58	81.01±0.67	74.47±0.86
GPR-GNN	64.85±0.27	44.88±0.34	86.24±0.61	72.94±0.97	55.48±0.91
JacobiConv	71.14±0.42	43.55±0.48	89.66±0.40	68.66±0.65	73.88±1.16
Our					
SONAR	**89.82**±0.57	52.22±0.14	**96.29**±0.73	83.57±1.44	74.96±1.10

Table 4: Sensitivity across different distances and recurrences in the Line-50 graph from Section 4.1.

	SONAR				GCN				
N. Recurrences→ / **Distance ↓**	**25**	**50**	**75**	**100**	**N. Recurrences→** / **Distance ↓**	**25** $\times 10^{-5}$	**50** $\times 10^{-5}$	**75** $\times 10^{-5}$	**100** $\times 10^{-5}$
10	0.0115	0.0413	0.573	1.955	**10**	0.7078	0.0	1.1470	0.3562
20	0.0037	0.0334	0.703	5.084	**20**	0.0	0.0	1.0490	0.2980
30	0.0273	0.0616	1.269	4.341	**30**	0.3725	0.9779	0.5259	0.0745
40	0.0131	0.0253	0.584	1.061	**40**	0.0	0.0	0.0	0.0
50	0.0002	0.0324	0.143	1.004	**50**	0.0	0.0	0.0	0.0

5 Conclusions

In this work, we introduced SONAR a novel DE-GNN architecture that models information propagation using wave dynamics governed by the graph wave equation. SONAR offers a principled approach for long-range information propagation by balancing conservative and non-conservative behaviors by integrating adaptive edge resistances and state-dependent external forces. Our theoretical analysis demonstrates that SONAR's energy preservation ensures stable and effective propagation of information over long distances. Moreover, the sensitivity analysis confirms that SONAR maintains non-vanishing influence between distant nodes, both in its continuous and discretized forms. Empirically, SONAR achieves state-of-the-art performance on a range of challenging benchmarks, i.e., synthetic and real-world long-range tasks, as well as heterophilic tasks. For such a reason, we believe SONAR represents a step forward in the design of GNNs capable of effective long-range propagation. Future work can focus on exploring alternative discretization methods, e.g., adaptive multistep scheme [4], and extend SONAR to temporal graphs [38].

Impact Statement. This work aims to advance the field of machine learning on graphs, with a focus on enhancing long-range information propagation. There are many potential societal consequences of our work, none which we feel must be specifically highlighted here.

Acknowledgments and Disclosure of Funding

The work has been partially supported by EU-EIC EMERGE (Grant No. 101070918).

References

[1] Sami Abu-El-Haija, Bryan Perozzi, Amol Kapoor, Nazanin Alipourfard, Kristina Lerman, Hrayr Harutyunyan, Greg Ver Steeg, and Aram Galstyan. Mixhop: Higher-order graph convolutional architectures via sparsified neighborhood mixing. In *International Conference on Machine Learning*, pages 21–29. PMLR, 2019.

[2] Uri Alon and Eran Yahav. On the Bottleneck of Graph Neural Networks and its Practical Implications. In *International Conference on Learning Representations*, 2021.

[3] Álvaro Arroyo, Alessio Gravina, Benjamin Gutteridge, Federico Barbero, Claudio Gallicchio, Xiaowen Dong, Michael Bronstein, and Pierre Vandergheynst. On vanishing gradients, over-smoothing, and over-squashing in gnns: Bridging recurrent and graph learning. *arXiv preprint arXiv:2502.10818*, 2025.

[4] Uri M. Ascher and Linda R. Petzold. *Computer Methods for Ordinary Differential Equations and Differential-Algebraic Equations*. Society for Industrial and Applied Mathematics, USA, 1st edition, 1998.

[5] Davide Bacciu, Federico Errica, Alessio Gravina, Lorenzo Madeddu, Marco Podda, and Giovanni Stilo. Deep Graph Networks for Drug Repurposing With Multi-Protein Targets. *IEEE Transactions on Emerging Topics in Computing*, 12(1):177–189, 2024.

[6] Jacob Bamberger, Benjamin Gutteridge, Scott le Roux, Michael M. Bronstein, and Xiaowen Dong. On measuring long-range interactions in graph neural networks. In *Forty-second International Conference on Machine Learning*, 2025.

[7] Federico Barbero, Ameya Velingker, Amin Saberi, Michael M. Bronstein, and Francesco Di Giovanni. Locality-aware graph rewiring in GNNs. In *The Twelfth International Conference on Learning Representations*, 2024.

[8] Deyu Bo, Xiao Wang, Chuan Shi, and Huawei Shen. Beyond low-frequency information in graph convolutional networks. *Proceedings of the AAAI Conference on Artificial Intelligence*, 35(5):3950–3957, May 2021.

[9] Xavier Bresson and Thomas Laurent. Residual Gated Graph ConvNets. *arXiv preprint arXiv:1711.07553*, 2018.

[10] Joan Bruna, Wojciech Zaremba, Arthur Szlam, and Yann LeCun. Spectral networks and locally connected networks on graphs. *arXiv preprint arXiv:1312.6203*, 2014.

[11] Chen Cai and Yusu Wang. A note on over-smoothing for graph neural networks. *arXiv preprint arXiv:2006.13318*, 2020.

[12] Andrea Ceni, Alessio Gravina, Claudio Gallicchio, Davide Bacciu, Carola-Bibiane Schonlieb, and Moshe Eliasof. Message-Passing State-Space Models: Improving Graph Learning with Modern Sequence Modeling. *arXiv preprint arXiv:2505.18728*, 2025.

[13] Benjamin Paul Chamberlain, James Rowbottom, Maria Gorinova, Stefan Webb, Emanuele Rossi, and Michael M Bronstein. GRAND: Graph neural diffusion. In *International Conference on Machine Learning (ICML)*, pages 1407–1418. PMLR, 2021.

[14] Jinsong Chen, Kaiyuan Gao, Gaichao Li, and Kun He. NAGphormer: A tokenized graph transformer for node classification in large graphs. In *The Eleventh International Conference on Learning Representations*, 2023.

[15] Ming Chen, Zhewei Wei, Zengfeng Huang, Bolin Ding, and Yaliang Li. Simple and Deep Graph Convolutional Networks. In Hal Daumé III and Aarti Singh, editors, *Proceedings of the 37th International Conference on Machine Learning*, volume 119 of *Proceedings of Machine Learning Research*, pages 1725–1735. PMLR, 13–18 Jul 2020.

[16] Ricky T. Q. Chen, Yulia Rubanova, Jesse Bettencourt, and David K Duvenaud. Neural Ordinary Differential Equations. In S. Bengio, H. Wallach, H. Larochelle, K. Grauman, N. Cesa-Bianchi, and R. Garnett, editors, *Advances in Neural Information Processing Systems*, volume 31. Curran Associates, Inc., 2018.

[17] Eli Chien, Jianhao Peng, Pan Li, and Olgica Milenkovic. Adaptive universal generalized pagerank graph neural network. In *International Conference on Learning Representations*, 2021.

[18] Michaël Defferrard, Xavier Bresson, and Pierre Vandergheynst. Convolutional Neural Networks on Graphs with Fast Localized Spectral Filtering. In *Advances in Neural Information Processing Systems*, volume 29. Curran Associates, Inc., 2016.

[19] Francesco Di Giovanni, Lorenzo Giusti, Federico Barbero, Giulia Luise, Pietro Liò, and Michael Bronstein. On over-squashing in message passing neural networks: the impact of width, depth, and topology. In *Proceedings of the 40th International Conference on Machine Learning*, ICML'23. JMLR.org, 2023.

[20] Yuhui Ding, Antonio Orvieto, Bobby He, and Thomas Hofmann. Recurrent distance filtering for graph representation learning. In *Forty-first International Conference on Machine Learning*, 2024.

[21] Yuhui Ding, Antonio Orvieto, Bobby He, and Thomas Hofmann. Recurrent distance filtering for graph representation learning. In Ruslan Salakhutdinov, Zico Kolter, Katherine Heller, Adrian Weller, Nuria Oliver, Jonathan Scarlett, and Felix Berkenkamp, editors, *Proceedings of the 41st International Conference on Machine Learning*, volume 235 of *Proceedings of Machine Learning Research*, pages 11002–11015. PMLR, 21–27 Jul 2024.

[22] Lun Du, Xiaozhou Shi, Qiang Fu, Xiaojun Ma, Hengyu Liu, Shi Han, and Dongmei Zhang. Gbk-gnn: Gated bi-kernel graph neural networks for modeling both homophily and heterophily. In *Proceedings of the ACM Web Conference 2022*, WWW '22, page 1550–1558, New York, NY, USA, 2022. Association for Computing Machinery.

[23] Vijay Prakash Dwivedi and Xavier Bresson. A Generalization of Transformer Networks to Graphs. *AAAI Workshop on Deep Learning on Graphs: Methods and Applications*, 2021.

[24] Vijay Prakash Dwivedi, Ladislav Rampášek, Michael Galkin, Ali Parviz, Guy Wolf, Anh Tuan Luu, and Dominique Beaini. Long Range Graph Benchmark. In *Advances in Neural Information Processing Systems*, volume 35, pages 22326–22340. Curran Associates, Inc., 2022.

[25] Moshe Eliasof, Alessio Gravina, Andrea Ceni, Claudio Gallicchio, Davide Bacciu, and Carola-Bibiane Schönlieb. Graph Adaptive Autoregressive Moving Average Models. In *Forty-second International Conference on Machine Learning*, 2025.

[26] Moshe Eliasof, Eldad Haber, and Eran Treister. PDE-GCN: Novel Architectures for Graph Neural Networks Motivated by Partial Differential Equations. In *Advances in Neural Information Processing Systems*, volume 34, pages 3836–3849. Curran Associates, Inc., 2021.

[27] Moshe Eliasof, Eldad Haber, Eran Treister, and Carola-Bibiane B Schönlieb. On The Temporal Domain of Differential Equation Inspired Graph Neural Networks. In *Proceedings of The 27th International Conference on Artificial Intelligence and Statistics*, volume 238 of *Proceedings of Machine Learning Research*, pages 1792–1800. PMLR, 02–04 May 2024.

[28] Federico Errica, Henrik Christiansen, Viktor Zaverkin, Takashi Maruyama, Mathias Niepert, and Francesco Alesiani. Adaptive message passing: A general framework to mitigate oversmoothing, oversquashing, and underreaching. *arXiv preprint arXiv:2312.16560*, 2024.

[29] Lawrence C Evans. *Partial Differential Equations*. Graduate studies in mathematics. American Mathematical Society, Providence, RI, 2 edition, March 2010.

[30] Maurice Ewing and J. Lamar Worzel. Long-range sound transmission. In *Propagation of Sound in the Ocean*. Geological Society of America, 01 1948.

[31] Joel H Ferziger and Milovan Peric. *Computational methods for fluid dynamics*. Springer, Berlin, Germany, 3 edition, November 2001.

[32] Ben Finkelshtein, Xingyue Huang, Michael M. Bronstein, and Ismail Ilkan Ceylan. Cooperative Graph Neural Networks. In *Forty-first International Conference on Machine Learning*, 2024.

[33] Joel Friedman and Jean-Pierre Tillich. Calculus on graphs. *ArXiv*, cs.DM/0408028, 2004.

[34] Joel Friedman and Jean-Pierre Tillich. Wave equations for graphs and the edge-based laplacian. *Pacific J. Math.*, 216(2):229–266, October 2004.

[35] Johannes Gasteiger, Stefan Weiß enberger, and Stephan Günnemann. Diffusion Improves Graph Learning. In *Advances in Neural Information Processing Systems*, volume 32. Curran Associates, Inc., 2019.

[36] Justin Gilmer, Samuel S. Schoenholz, Patrick F. Riley, Oriol Vinyals, and George E. Dahl. Neural message passing for Quantum chemistry. In *Proceedings of the 34th International Conference on Machine Learning*, volume 70 of *ICML'17*, page 1263–1272. JMLR.org, 2017.

[37] Francesco Di Giovanni, James Rowbottom, Benjamin Paul Chamberlain, Thomas Markovich, and Michael M. Bronstein. Understanding convolution on graphs via energies. *Transactions on Machine Learning Research*, 2023.

[38] Alessio Gravina and Davide Bacciu. Deep Learning for Dynamic Graphs: Models and Benchmarks. *IEEE Transactions on Neural Networks and Learning Systems*, 35(9):11788–11801, 2024.

[39] Alessio Gravina, Davide Bacciu, and Claudio Gallicchio. Anti-Symmetric DGN: a stable architecture for Deep Graph Networks. In *The Eleventh International Conference on Learning Representations*, 2023.

[40] Alessio Gravina, Moshe Eliasof, Claudio Gallicchio, Davide Bacciu, and Carola-Bibiane Schönlieb. On Oversquashing in Graph Neural Networks Through the Lens of Dynamical Systems. *Proceedings of the AAAI Conference on Artificial Intelligence*, 39(16):16906–16914, Apr. 2025.

[41] Alessio Gravina, Claudio Gallicchio, and Davide Bacciu. Non-dissipative Propagation by Randomized Anti-symmetric Deep Graph Networks. In *Machine Learning and Principles and Practice of Knowledge Discovery in Databases*, pages 25–36, Cham, 2025. Springer Nature Switzerland.

[42] Alessio Gravina, Giulio Lovisotto, Claudio Gallicchio, Davide Bacciu, and Claas Grohnfeldt. Long Range Propagation on Continuous-Time Dynamic Graphs. In *Proceedings of the 41st International Conference on Machine Learning*, volume 235 of *Proceedings of Machine Learning Research*, pages 16206–16225. PMLR, 21–27 Jul 2024.

[43] Alessio Gravina, Jennifer L. Wilson, Davide Bacciu, Kevin J. Grimes, and Corrado Priami. Controlling astrocyte-mediated synaptic pruning signals for schizophrenia drug repurposing with deep graph networks. *PLOS Computational Biology*, 18(5):1–19, 05 2022.

[44] Alessio Gravina, Daniele Zambon, Davide Bacciu, and Cesare Alippi. Temporal graph odes for irregularly-sampled time series. In Kate Larson, editor, *Proceedings of the Thirty-Third International Joint Conference on Artificial Intelligence, IJCAI-24*, pages 4025–4034. International Joint Conferences on Artificial Intelligence Organization, 8 2024.

[45] Albert Gu, Karan Goel, and Christopher Ré. Efficiently modeling long sequences with structured state spaces. *arXiv preprint arXiv:2111.00396*, 2021.

[46] Benjamin Gutteridge, Xiaowen Dong, Michael M Bronstein, and Francesco Di Giovanni. Drew: Dynamically rewired message passing with delay. In *International Conference on Machine Learning*, pages 12252–12267. PMLR, 2023.

[47] E. Haber and L. Ruthotto. Stable architectures for deep neural networks. *Inverse Problems*, 34(1), 2017.

[48] Donald E Hall. *Musical Acoustics*. Brooks/Cole, Florence, KY, January 1980.

[49] William L. Hamilton, Rex Ying, and Jure Leskovec. Inductive representation learning on large graphs. In *Proceedings of the 31st International Conference on Neural Information Processing Systems*, NIPS'17, page 1025–1035. Curran Associates Inc., 2017.

[50] Andi Han, Dai Shi, Lequan Lin, and Junbin Gao. From Continuous Dynamics to Graph Neural Networks: Neural Diffusion and Beyond. *Transactions on Machine Learning Research*, 2024. Survey Certification.

[51] Xiaoxin He, Bryan Hooi, Thomas Laurent, Adam Perold, Yann LeCun, and Xavier Bresson. A generalization of vit/mlp-mixer to graphs. In *Proceedings of the 40th International Conference on Machine Learning*, ICML'23, 2023.

[52] Simon Heilig, Alessio Gravina, Alessandro Trenta, Claudio Gallicchio, and Davide Bacciu. Port-Hamiltonian Architectural Bias for Long-Range Propagation in Deep Graph Networks. In *The Thirteenth International Conference on Learning Representations*, 2025.

[53] Matthias Hein, Jean-Yves Audibert, and Ulrike von Luxburg. Graph laplacians and their convergence on random neighborhood graphs. *Journal of Machine Learning Research*, 8(48):1325–1368, 2007.

[54] Weihua Hu, Bowen Liu, Joseph Gomes, Marinka Zitnik, Percy Liang, Vijay Pande, and Jure Leskovec. Strategies for Pre-training Graph Neural Networks. In *International Conference on Learning Representations*, 2020.

[55] Ming Jin, Yu Zheng, Yuan-Fang Li, Siheng Chen, Bin Yang, and Shirui Pan. Multivariate time series forecasting with dynamic graph neural odes. *IEEE Transactions on Knowledge and Data Engineering*, 2022.

[56] Qiyu Kang, Kai Zhao, Yang Song, Sijie Wang, and Wee Peng Tay. Node Embedding from Neural Hamiltonian Orbits in Graph Neural Networks. In *Proceedings of the 40th International Conference on Machine Learning*, volume 202 of *Proceedings of Machine Learning Research*, pages 15786–15808. PMLR, 23–29 Jul 2023.

[57] Kedar Karhadkar, Pradeep Kr. Banerjee, and Guido Montufar. FoSR: First-order spectral rewiring for addressing oversquashing in GNNs. In *The Eleventh International Conference on Learning Representations*, 2023.

[58] Bharti Khemani, Shruti Patil, Ketan Kotecha, and Sudeep Tanwar. A review of graph neural networks: concepts, architectures, techniques, challenges, datasets, applications, and future directions. *Journal of Big Data*, 11(1):18, Jan 2024.

[59] Thomas N. Kipf and Max Welling. Semi-Supervised Classification with Graph Convolutional Networks. In *International Conference on Learning Representations*, 2017.

[60] Kezhi Kong, Jiuhai Chen, John Kirchenbauer, Renkun Ni, C. Bayan Bruss, and Tom Goldstein. GOAT: A global transformer on large-scale graphs. In Andreas Krause, Emma Brunskill, Kyunghyun Cho, Barbara Engelhardt, Sivan Sabato, and Jonathan Scarlett, editors, *Proceedings of the 40th International Conference on Machine Learning*, volume 202 of *Proceedings of Machine Learning Research*, pages 17375–17390. PMLR, 23–29 Jul 2023.

[61] Devin Kreuzer, Dominique Beaini, Will Hamilton, Vincent Létourneau, and Prudencio Tossou. Rethinking graph transformers with spectral attention. *Advances in Neural Information Processing Systems*, 34:21618–21629, 2021.

[62] L D Landau and E M Lifshitz. *Mechanics and electrodynamics*. Elsevier, October 2013.

[63] Xiang Li, Renyu Zhu, Yao Cheng, Caihua Shan, Siqiang Luo, Dongsheng Li, and Weining Qian. Finding global homophily in graph neural networks when meeting heterophily. In Kamalika Chaudhuri, Stefanie Jegelka, Le Song, Csaba Szepesvari, Gang Niu, and Sivan Sabato, editors, *Proceedings of the 39th International Conference on Machine Learning*, volume 162 of *Proceedings of Machine Learning Research*, pages 13242–13256. PMLR, 17–23 Jul 2022.

[64] Sitao Luan, Chenqing Hua, Qincheng Lu, Liheng Ma, Lirong Wu, Xinyu Wang, Minkai Xu, Xiao-Wen Chang, Doina Precup, Rex Ying, Stan Z. Li, Jian Tang, Guy Wolf, and Stefanie Jegelka. The heterophilic graph learning handbook: Benchmarks, models, theoretical analysis, applications and challenges. *arXiv preprint arXiv:2407.09618*, 2024.

[65] Liheng Ma, Chen Lin, Derek Lim, Adriana Romero-Soriano, Puneet K. Dokania, Mark Coates, Philip Torr, and Ser-Nam Lim. Graph inductive biases in transformers without message passing. In *Proceedings of the 40th International Conference on Machine Learning*, volume 202 of *Proceedings of Machine Learning Research*, pages 23321–23337. PMLR, 23–29 Jul 2023.

[66] Sunil Kumar Maurya, Xin Liu, and Tsuyoshi Murata. Simplifying approach to node classification in graph neural networks. *Journal of Computational Science*, 62:101695, 2022.

[67] Alessio Micheli. Neural Network for Graphs: A Contextual Constructive Approach. *IEEE Transactions on Neural Networks*, 20(3):498–511, 2009.

[68] Kenta Oono and Taiji Suzuki. Graph Neural Networks Exponentially Lose Expressive Power for Node Classification. In *International Conference on Learning Representations*, 2020.

[69] Antonio Orvieto, Samuel L Smith, Albert Gu, Anushan Fernando, Caglar Gulcehre, Razvan Pascanu, and Soham De. Resurrecting recurrent neural networks for long sequences. In *International Conference on Machine Learning*, pages 26670–26698. PMLR, 2023.

[70] Oleg Platonov, Denis Kuznedelev, Michael Diskin, Artem Babenko, and Liudmila Prokhorenkova. A critical look at the evaluation of GNNs under heterophily: Are we really making progress? In *The Eleventh International Conference on Learning Representations*, 2023.

[71] Michael Poli, Stefano Massaroli, Junyoung Park, Atsushi Yamashita, Hajime Asama, and Jinkyoo Park. Graph neural ordinary differential equations. *arXiv preprint arXiv:1911.07532*, 2019.

[72] Ladislav Rampášek, Mikhail Galkin, Vijay Prakash Dwivedi, Anh Tuan Luu, Guy Wolf, and Dominique Beaini. Recipe for a General, Powerful, Scalable Graph Transformer. *Advances in Neural Information Processing Systems*, 35, 2022.

[73] T. Konstantin Rusch, Michael M. Bronstein, and Siddhartha Mishra. A Survey on Oversmoothing in Graph Neural Networks. *arXiv preprint arXiv:2303.10993*, 2023.

[74] T Konstantin Rusch, Ben Chamberlain, James Rowbottom, Siddhartha Mishra, and Michael Bronstein. Graph-coupled oscillator networks. In *International Conference on Machine Learning*, pages 18888–18909. PMLR, 2022.

[75] T Konstantin Rusch, Ben Chamberlain, James Rowbottom, Siddhartha Mishra, and Michael Bronstein. Graph-coupled oscillator networks. In *International Conference on Machine Learning*, pages 18888–18909. PMLR, 2022.

[76] Franco Scarselli, Marco Gori, Ah Chung Tsoi, Markus Hagenbuchner, and Gabriele Monfardini. The Graph Neural Network Model. *IEEE Transactions on Neural Networks*, 20(1):61–80, 2009.

[77] Dai Shi, Andi Han, Lequan Lin, Yi Guo, and Junbin Gao. Exposition on over-squashing problem on GNNs: Current Methods, Benchmarks and Challenges, 2023.

[78] Yunsheng Shi, Zhengjie Huang, Shikun Feng, Hui Zhong, Wenjing Wang, and Yu Sun. Masked Label Prediction: Unified Message Passing Model for Semi-Supervised Classification. In *Proceedings of the Thirtieth International Joint Conference on Artificial Intelligence, IJCAI-21*, pages 1548–1554. International Joint Conferences on Artificial Intelligence Organization, 8 2021.

[79] Yunsheng Shi, Zhengjie Huang, Shikun Feng, Hui Zhong, Wenjing Wang, and Yu Sun. Masked label prediction: Unified message passing model for semi-supervised classification. In Zhi-Hua Zhou, editor, *Proceedings of the Thirtieth International Joint Conference on Artificial Intelligence, IJCAI-21*, pages 1548–1554. International Joint Conferences on Artificial Intelligence Organization, 8 2021. Main Track.

[80] Hamed Shirzad, Ameya Velingker, Balaji Venkatachalam, Danica J Sutherland, and Ali Kemal Sinop. Exphormer: Sparse transformers for graphs. In *International Conference on Machine Learning*, pages 31613–31632. PMLR, 2023.

[81] Matthew Thorpe, Tan Minh Nguyen, Hedi Xia, Thomas Strohmer, Andrea Bertozzi, Stanley Osher, and Bao Wang. GRAND++: Graph Neural Diffusion with A Source Term. In *International Conference on Learning Representations*, 2022.

[82] Jan Tönshoff, Martin Ritzert, Eran Rosenbluth, and Martin Grohe. Where did the gap go? reassessing the long-range graph benchmark. In *The Second Learning on Graphs Conference*, 2023.

[83] Jake Topping, Francesco Di Giovanni, Benjamin Paul Chamberlain, Xiaowen Dong, and Michael M. Bronstein. Understanding over-squashing and bottlenecks on graphs via curvature. In *International Conference on Learning Representations*, 2022.

[84] A. Vaswani et al. Attention is all you need. *Advances in Neural Information Processing Systems*, 30, 2017.

[85] Petar Veličković, Guillem Cucurull, Arantxa Casanova, Adriana Romero, Pietro Liò, and Yoshua Bengio. Graph Attention Networks. In *International Conference on Learning Representations*, 2018.

[86] Xiyuan Wang and Muhan Zhang. How powerful are spectral graph neural networks. In Kamalika Chaudhuri, Stefanie Jegelka, Le Song, Csaba Szepesvari, Gang Niu, and Sivan Sabato, editors, *Proceedings of the 39th International Conference on Machine Learning*, volume 162 of *Proceedings of Machine Learning Research*, pages 23341–23362. PMLR, 17–23 Jul 2022.

[87] Yifei Wang, Yisen Wang, Jiansheng Yang, and Zhouchen Lin. Dissecting the Diffusion Process in Linear Graph Convolutional Networks. In *Advances in Neural Information Processing Systems*, volume 34, pages 5758–5769. Curran Associates, Inc., 2021.

[88] Qitian Wu, Chenxiao Yang, Wentao Zhao, Yixuan He, David Wipf, and Junchi Yan. DIFFormer: Scalable (Graph) Transformers Induced by Energy Constrained Diffusion. In *The Eleventh International Conference on Learning Representations*, 2023.

[89] Keyulu Xu, Weihua Hu, Jure Leskovec, and Stefanie Jegelka. How Powerful are Graph Neural Networks? In *International Conference on Learning Representations*, 2019.

[90] Chengxuan Ying, Tianle Cai, Shengjie Luo, Shuxin Zheng, Guolin Ke, Di He, Yanming Shen, and Tie-Yan Liu. Do transformers really perform badly for graph representation? *Advances in Neural Information Processing Systems*, 34:28877–28888, 2021.

[91] Kai Zhao, Qiyu Kang, Yang Song, Rui She, Sijie Wang, and Wee Peng Tay. Adversarial robustness in graph neural networks: A hamiltonian approach. In *Advances in Neural Information Processing Systems*, volume 36, pages 3338–3361. Curran Associates, Inc., 2023.

[92] Jiong Zhu, Ryan A. Rossi, Anup Rao, Tung Mai, Nedim Lipka, Nesreen K. Ahmed, and Danai Koutra. Graph neural networks with heterophily. *Proceedings of the AAAI Conference on Artificial Intelligence*, 35(12):11168–11176, May 2021.

[93] Jiong Zhu, Yujun Yan, Lingxiao Zhao, Mark Heimann, Leman Akoglu, and Danai Koutra. Beyond homophily in graph neural networks: Current limitations and effective designs. In H. Larochelle, M. Ranzato, R. Hadsell, M.F. Balcan, and H. Lin, editors, *Advances in Neural Information Processing Systems*, volume 33, pages 7793–7804. Curran Associates, Inc., 2020.

NeurIPS Paper Checklist

1. **Claims**

   Question: Do the main claims made in the abstract and introduction accurately reflect the paper's contributions and scope?

   Answer: [Yes]

   Justification: All claims made in the abstract and the introduction are carefully explained and theoretically proven in Section 3. We included results on energy conservation and the long-range propagation capabilities through the sensitivity matrix in Section 3.3. Our experimental results in Section 4 reflect our theoretical findings and show the capabilities of our model on different tasks, including heterophilic and long-range tasks

   Guidelines:

   - The answer NA means that the abstract and introduction do not include the claims made in the paper.
   - The abstract and/or introduction should clearly state the claims made, including the contributions made in the paper and important assumptions and limitations. A No or NA answer to this question will not be perceived well by the reviewers.
   - The claims made should match theoretical and experimental results, and reflect how much the results can be expected to generalize to other settings.
   - It is fine to include aspirational goals as motivation as long as it is clear that these goals are not attained by the paper.

2. **Limitations**

   Question: Does the paper discuss the limitations of the work performed by the authors?

   Answer: [Yes]

   Justification: We discussed the limitations of our work in Appendix D.

   Guidelines:

   - The answer NA means that the paper has no limitation while the answer No means that the paper has limitations, but those are not discussed in the paper.
   - The authors are encouraged to create a separate "Limitations" section in their paper.
   - The paper should point out any strong assumptions and how robust the results are to violations of these assumptions (e.g., independence assumptions, noiseless settings, model well-specification, asymptotic approximations only holding locally). The authors should reflect on how these assumptions might be violated in practice and what the implications would be.
   - The authors should reflect on the scope of the claims made, e.g., if the approach was only tested on a few datasets or with a few runs. In general, empirical results often depend on implicit assumptions, which should be articulated.
   - The authors should reflect on the factors that influence the performance of the approach. For example, a facial recognition algorithm may perform poorly when image resolution is low or images are taken in low lighting. Or a speech-to-text system might not be used reliably to provide closed captions for online lectures because it fails to handle technical jargon.
   - The authors should discuss the computational efficiency of the proposed algorithms and how they scale with dataset size.
   - If applicable, the authors should discuss possible limitations of their approach to address problems of privacy and fairness.
   - While the authors might fear that complete honesty about limitations might be used by reviewers as grounds for rejection, a worse outcome might be that reviewers discover limitations that aren't acknowledged in the paper. The authors should use their best judgment and recognize that individual actions in favor of transparency play an important role in developing norms that preserve the integrity of the community. Reviewers will be specifically instructed to not penalize honesty concerning limitations.

3. **Theory assumptions and proofs**

Question: For each theoretical result, does the paper provide the full set of assumptions and a complete (and correct) proof?

Answer: [Yes]

Justification: Each theoretical result is carefully described and explained in Section 3.3, along with its consequences in theory and practice. Each of them has its proof in Appendix B, where we include additional statements.

Guidelines:

- The answer NA means that the paper does not include theoretical results.
- All the theorems, formulas, and proofs in the paper should be numbered and cross-referenced.
- All assumptions should be clearly stated or referenced in the statement of any theorems.
- The proofs can either appear in the main paper or the supplemental material, but if they appear in the supplemental material, the authors are encouraged to provide a short proof sketch to provide intuition.
- Inversely, any informal proof provided in the core of the paper should be complemented by formal proofs provided in appendix or supplemental material.
- Theorems and Lemmas that the proof relies upon should be properly referenced.

4. **Experimental result reproducibility**

Question: Does the paper fully disclose all the information needed to reproduce the main experimental results of the paper to the extent that it affects the main claims and/or conclusions of the paper (regardless of whether the code and data are provided or not)?

Answer: [Yes]

Justification: Section 3 describes all the details on the methodology and its practical implementation (i.e., , how to discretize the continuous process and write it in an MPNN-like form). Furthermore, all of our experiments are based on open-source datasets available online. The setup of each experiment is described in Section 4. Hyperparameters and additional details for performing experiments are described in Appendix A

Guidelines:

- The answer NA means that the paper does not include experiments.
- If the paper includes experiments, a No answer to this question will not be perceived well by the reviewers: Making the paper reproducible is important, regardless of whether the code and data are provided or not.
- If the contribution is a dataset and/or model, the authors should describe the steps taken to make their results reproducible or verifiable.
- Depending on the contribution, reproducibility can be accomplished in various ways. For example, if the contribution is a novel architecture, describing the architecture fully might suffice, or if the contribution is a specific model and empirical evaluation, it may be necessary to either make it possible for others to replicate the model with the same dataset, or provide access to the model. In general. releasing code and data is often one good way to accomplish this, but reproducibility can also be provided via detailed instructions for how to replicate the results, access to a hosted model (e.g., in the case of a large language model), releasing of a model checkpoint, or other means that are appropriate to the research performed.
- While NeurIPS does not require releasing code, the conference does require all submissions to provide some reasonable avenue for reproducibility, which may depend on the nature of the contribution. For example
  (a) If the contribution is primarily a new algorithm, the paper should make it clear how to reproduce that algorithm.
  (b) If the contribution is primarily a new model architecture, the paper should describe the architecture clearly and fully.
  (c) If the contribution is a new model (e.g., a large language model), then there should either be a way to access this model for reproducing the results or a way to reproduce the model (e.g., with an open-source dataset or instructions for how to construct the dataset).

(d) We recognize that reproducibility may be tricky in some cases, in which case authors are welcome to describe the particular way they provide for reproducibility. In the case of closed-source models, it may be that access to the model is limited in some way (e.g., to registered users), but it should be possible for other researchers to have some path to reproducing or verifying the results.

5. **Open access to data and code**

   Question: Does the paper provide open access to the data and code, with sufficient instructions to faithfully reproduce the main experimental results, as described in supplemental material?

   Answer: [Yes]

   Justification: We provide all the details to implement the main method in Section 3, as well as describing the setup for each experiment in Section 4 and Appendix A, providing sufficient information to reproduce our experiments. Moreover, all our experiments fully rely on public benchmarks. We openly release the code to reproduce our empirical evaluation upon acceptance.

   Guidelines:

   - The answer NA means that paper does not include experiments requiring code.
   - Please see the NeurIPS code and data submission guidelines (`https://nips.cc/public/guides/CodeSubmissionPolicy`) for more details.
   - While we encourage the release of code and data, we understand that this might not be possible, so "No" is an acceptable answer. Papers cannot be rejected simply for not including code, unless this is central to the contribution (e.g., for a new open-source benchmark).
   - The instructions should contain the exact command and environment needed to run to reproduce the results. See the NeurIPS code and data submission guidelines (`https://nips.cc/public/guides/CodeSubmissionPolicy`) for more details.
   - The authors should provide instructions on data access and preparation, including how to access the raw data, preprocessed data, intermediate data, and generated data, etc.
   - The authors should provide scripts to reproduce all experimental results for the new proposed method and baselines. If only a subset of experiments are reproducible, they should state which ones are omitted from the script and why.
   - At submission time, to preserve anonymity, the authors should release anonymized versions (if applicable).
   - Providing as much information as possible in supplemental material (appended to the paper) is recommended, but including URLs to data and code is permitted.

6. **Experimental setting/details**

   Question: Does the paper specify all the training and test details (e.g., data splits, hyperparameters, how they were chosen, type of optimizer, etc.) necessary to understand the results?

   Answer: [Yes]

   Justification: The setup of each experiment is described in Section 4. For each of them, we provide a reference to the original paper that described and analyzed these datasets and tasks. Hyperparameters for each task are available in Appendix A.4.

   Guidelines:

   - The answer NA means that the paper does not include experiments.
   - The experimental setting should be presented in the core of the paper to a level of detail that is necessary to appreciate the results and make sense of them.
   - The full details can be provided either with the code, in appendix, or as supplemental material.

7. **Experiment statistical significance**

   Question: Does the paper report error bars suitably and correctly defined or other appropriate information about the statistical significance of the experiments?

Answer: [Yes]

Justification: The experiments for Graph Property Prediction, Graph Transfer, and Long-Range Graph Benchmark are all performed with 3 or 4 different seeds, and the results are provided with the average between runs and the standard deviation to verify the significance of results. Experiments with heterophilic graphs are performed with 10 folds each, and results are provided in the same way.

Guidelines:

- The answer NA means that the paper does not include experiments.
- The authors should answer "Yes" if the results are accompanied by error bars, confidence intervals, or statistical significance tests, at least for the experiments that support the main claims of the paper.
- The factors of variability that the error bars are capturing should be clearly stated (for example, train/test split, initialization, random drawing of some parameter, or overall run with given experimental conditions).
- The method for calculating the error bars should be explained (closed form formula, call to a library function, bootstrap, etc.)
- The assumptions made should be given (e.g., Normally distributed errors).
- It should be clear whether the error bar is the standard deviation or the standard error of the mean.
- It is OK to report 1-sigma error bars, but one should state it. The authors should preferably report a 2-sigma error bar than state that they have a 96% CI, if the hypothesis of Normality of errors is not verified.
- For asymmetric distributions, the authors should be careful not to show in tables or figures symmetric error bars that would yield results that are out of range (e.g. negative error rates).
- If error bars are reported in tables or plots, The authors should explain in the text how they were calculated and reference the corresponding figures or tables in the text.

8. **Experiments compute resources**

   Question: For each experiment, does the paper provide sufficient information on the computer resources (type of compute workers, memory, time of execution) needed to reproduce the experiments?

   Answer: [Yes]

   Justification: We provide details on the experimental setup in Section 4 and Appendix A. A comparison of the computational time and resources required to perform experiments is available in Table 11.

   Guidelines:

   - The answer NA means that the paper does not include experiments.
   - The paper should indicate the type of compute workers CPU or GPU, internal cluster, or cloud provider, including relevant memory and storage.
   - The paper should provide the amount of compute required for each of the individual experimental runs as well as estimate the total compute.
   - The paper should disclose whether the full research project required more compute than the experiments reported in the paper (e.g., preliminary or failed experiments that didn't make it into the paper).

9. **Code of ethics**

   Question: Does the research conducted in the paper conform, in every respect, with the NeurIPS Code of Ethics `https://neurips.cc/public/EthicsGuidelines`?

   Answer: [Yes]

   Justification: The research conducted in this paper conforms in every aspect with the NeurIPS Code of Ethics. Our research does not involve sensitive data or human subjects, nor idoes t represent a potential harm for society.

   Guidelines:

- The answer NA means that the authors have not reviewed the NeurIPS Code of Ethics.
- If the authors answer No, they should explain the special circumstances that require a deviation from the Code of Ethics.
- The authors should make sure to preserve anonymity (e.g., if there is a special consideration due to laws or regulations in their jurisdiction).

10. **Broader impacts**

    Question: Does the paper discuss both potential positive societal impacts and negative societal impacts of the work performed?

    Answer: [Yes]

    Justification: We discuss potential impacts after the conclusion.

    Guidelines:

    - The answer NA means that there is no societal impact of the work performed.
    - If the authors answer NA or No, they should explain why their work has no societal impact or why the paper does not address societal impact.
    - Examples of negative societal impacts include potential malicious or unintended uses (e.g., disinformation, generating fake profiles, surveillance), fairness considerations (e.g., deployment of technologies that could make decisions that unfairly impact specific groups), privacy considerations, and security considerations.
    - The conference expects that many papers will be foundational research and not tied to particular applications, let alone deployments. However, if there is a direct path to any negative applications, the authors should point it out. For example, it is legitimate to point out that an improvement in the quality of generative models could be used to generate deepfakes for disinformation. On the other hand, it is not needed to point out that a generic algorithm for optimizing neural networks could enable people to train models that generate Deepfakes faster.
    - The authors should consider possible harms that could arise when the technology is being used as intended and functioning correctly, harms that could arise when the technology is being used as intended but gives incorrect results, and harms following from (intentional or unintentional) misuse of the technology.
    - If there are negative societal impacts, the authors could also discuss possible mitigation strategies (e.g., gated release of models, providing defenses in addition to attacks, mechanisms for monitoring misuse, mechanisms to monitor how a system learns from feedback over time, improving the efficiency and accessibility of ML).

11. **Safeguards**

    Question: Does the paper describe safeguards that have been put in place for responsible release of data or models that have a high risk for misuse (e.g., pretrained language models, image generators, or scraped datasets)?

    Answer: [NA]

    Justification: The paper poses no particular risk of misuse for the models and datasets employed.

    Guidelines:

    - The answer NA means that the paper poses no such risks.
    - Released models that have a high risk for misuse or dual-use should be released with necessary safeguards to allow for controlled use of the model, for example by requiring that users adhere to usage guidelines or restrictions to access the model or implementing safety filters.
    - Datasets that have been scraped from the Internet could pose safety risks. The authors should describe how they avoided releasing unsafe images.
    - We recognize that providing effective safeguards is challenging, and many papers do not require this, but we encourage authors to take this into account and make a best faith effort.

12. **Licenses for existing assets**

Question: Are the creators or original owners of assets (e.g., code, data, models), used in the paper, properly credited and are the license and terms of use explicitly mentioned and properly respected?

Answer: [Yes]

Justification: For each dataset and task used in this work, we correctly cite and mention the work introducing it and relevant related studies. Licenses and terms of use are properly respected.

Guidelines:

- The answer NA means that the paper does not use existing assets.
- The authors should cite the original paper that produced the code package or dataset.
- The authors should state which version of the asset is used and, if possible, include a URL.
- The name of the license (e.g., CC-BY 4.0) should be included for each asset.
- For scraped data from a particular source (e.g., website), the copyright and terms of service of that source should be provided.
- If assets are released, the license, copyright information, and terms of use in the package should be provided. For popular datasets, `paperswithcode.com/datasets` has curated licenses for some datasets. Their licensing guide can help determine the license of a dataset.
- For existing datasets that are re-packaged, both the original license and the license of the derived asset (if it has changed) should be provided.
- If this information is not available online, the authors are encouraged to reach out to the asset's creators.

13. **New assets**

Question: Are new assets introduced in the paper well documented and is the documentation provided alongside the assets?

Answer: [NA]

Justification: This paper does not release new assets.

Guidelines:

- The answer NA means that the paper does not release new assets.
- Researchers should communicate the details of the dataset/code/model as part of their submissions via structured templates. This includes details about training, license, limitations, etc.
- The paper should discuss whether and how consent was obtained from people whose asset is used.
- At submission time, remember to anonymize your assets (if applicable). You can either create an anonymized URL or include an anonymized zip file.

14. **Crowdsourcing and research with human subjects**

Question: For crowdsourcing experiments and research with human subjects, does the paper include the full text of instructions given to participants and screenshots, if applicable, as well as details about compensation (if any)?

Answer: [NA]

Justification: This work does not involve any crowdsourcing or research with human subjects.

Guidelines:

- The answer NA means that the paper does not involve crowdsourcing nor research with human subjects.
- Including this information in the supplemental material is fine, but if the main contribution of the paper involves human subjects, then as much detail as possible should be included in the main paper.
- According to the NeurIPS Code of Ethics, workers involved in data collection, curation, or other labor should be paid at least the minimum wage in the country of the data collector.

15. **Institutional review board (IRB) approvals or equivalent for research with human subjects**

    Question: Does the paper describe potential risks incurred by study participants, whether such risks were disclosed to the subjects, and whether Institutional Review Board (IRB) approvals (or an equivalent approval/review based on the requirements of your country or institution) were obtained?

    Answer: [NA]

    Justification: This work does not involve any crowdsourcing or research with human subjects.

    Guidelines:

    - The answer NA means that the paper does not involve crowdsourcing nor research with human subjects.
    - Depending on the country in which research is conducted, IRB approval (or equivalent) may be required for any human subjects research. If you obtained IRB approval, you should clearly state this in the paper.
    - We recognize that the procedures for this may vary significantly between institutions and locations, and we expect authors to adhere to the NeurIPS Code of Ethics and the guidelines for their institution.
    - For initial submissions, do not include any information that would break anonymity (if applicable), such as the institution conducting the review.

16. **Declaration of LLM usage**

    Question: Does the paper describe the usage of LLMs if it is an important, original, or non-standard component of the core methods in this research? Note that if the LLM is used only for writing, editing, or formatting purposes and does not impact the core methodology, scientific rigorousness, or originality of the research, declaration is not required.

    Answer: [NA]

    Justification: The core method development in our research does not involve LLMs as any important, original or non-standard components.

    Guidelines:

    - The answer NA means that the core method development in this research does not involve LLMs as any important, original, or non-standard components.
    - Please refer to our LLM policy (`https://neurips.cc/Conferences/2025/LLM`) for what should or should not be described.

A Experimental Details

A.1 Edge Feature Aggregation

Together with the usual node features $\bar{\mathbf{x}}_v \in \mathbb{R}^d$, some graphs provide edge features $\mathbf{E} \in \mathbb{R}^{m \times d_e}$ made of a d_e-dimensional vector $\mathbf{e}_{uv} \in \mathbb{R}^{d_e}$ for every edge $(u, v) \in \mathcal{E}$. While classical MPNNs add this information during the convolution, we adopt a different approach to preserve our wave-like propagation and theoretical properties. In particular, we follow [26], transforming the edge features and injecting them into the node space. To do so, we define the average Avg and gradient Grad operators, which shift node features into edge features [26, 33], as

$$(\text{Avg}\mathbf{X})_{uv} = \frac{1}{2}\mathbf{G}_{uv}(\mathbf{x}_v + \mathbf{x}_u), \qquad (\text{Grad}\mathbf{X})_{uv} = \mathbf{G}_{uv}(\mathbf{x}_v - \mathbf{x}_u), \tag{14}$$

where $\mathbf{G} \in \mathbb{R}^{n \times n}$ is a matrix where $\mathbf{G}_{uv} = \frac{1}{\gamma_{uv}}$ and γ_{uv} is the geometric mean of the degrees of nodes u and v. Their adjoint operators, which coincide with their transpose, transform edge features into node features [33, 26]. Therefore, before starting the propagation of information, the initial condition is a concatenation of the initial node features and the transformation of the edge ones:

$$\bar{\mathbf{X}}_{\text{new}} = \left(\bar{\mathbf{X}} \oplus \text{Avg}^\top \mathbf{E} \oplus \text{Grad}^\top \mathbf{E}\right) \tag{15}$$

A.2 Employed Baselines

In our experiments, the performance of our method is compared with various state-of-the-art GNN baselines from the literature. Specifically, we consider:

- classical MPNN-based methods, i.e., GCN [59], GraphSAGE [49], GAT [85], GatedGCN [9], GIN [89], GINE [54], GCNII [15];
- heterophily-specific models, i.e., H2GCN [93], CPGNN [92], FAGCN [8], GPR-GNN [17], FSGNN [66], GloGNN [63], GBK-GNN [22], and JacobiConv [86];
- DE-GNNs, i.e., DGC [87], GRAND [13], GraphCON [75], A-DGN [39], SWAN [40], PH-DGN [52];
- Graph Transformers, i.e., Transformer [84, 23], GT [79], SAN [61], GPS [72], GOAT [60], Exphormer [80], NAGphormer [14], GRIT[65], and GraphViT [51];
- Higher-Order GNNs, i.e., DIGL [35], MixHop [1], DRew [46], and GRED [20]. .

A.3 Employed Datasets

In our experiments, we evaluate SONAR's performance on widely used graph benchmarks. Specifically, we consider long-range propagation tasks, including the graph transfer tasks from [40], as well as the three graph property prediction tasks introduced in [39] ("Diameter", "SSSP", and "Eccentricity"). Additionally, we assess SONAR on the "Peptide-func", "Peptide-struct", and "PascalVOC-SP" tasks from the real-world Long-Range Graph Benchmark (LRGB) [24]. To further evaluate its effectiveness, we include five heterophilic tasks: "Roman-empire", "Amazon-ratings", "Minesweeper", "Tolokers", and "Questions" [70]. We highlight that the three graph property prediction tasks are problems fundamentally linked with information propagation, as node signals must travel from each node v across the entire graph. Therefore, they require nodes to iteratively exchange information with increasingly distant nodes. This process shares similarities with classical algorithms like Bellman-Ford or Dijkstra's algorithm. Indeed, Dijkstra's algorithm works by progressively expanding a frontier of visited nodes, where each node updates the shortest known distance to its neighbors.

In Table 5, we report the statistics of the employed datasets.

A.4 Hyperparameter Space

The hyperparameter space employed by SONAR in our experiments is reported in Table 6.

Table 5: Dataset statistics.

Dataset	#Nodes	#Edges	#Graphs	Task
Graph Transfer	3 - 100	7 - 396	1,200	Node Regression
Diameter	25 - 35	22 - 553	7,040	Graph Regression
SSSP	25 - 35	22 - 553	7,040	Node Regression
Eccentricity	25 - 35	22 - 553	7,040	Node Regression
Peptide-func	8 - 444	10 - 928	15,535	Graph Classification
Peptide-struct	8 - 444	10 - 928	15,535	Graph Regression
PascalVOC-SP	198 - 500	1,044 - 2,942	11,355	Node Classification
Roman-empire	22,662	32,927	1	Node Classification
Amazon-ratings	24,492	93,050	1	Node Classification
Minesweeper	10,000	39,402	1	Node Classification
Tolokers	11,758	519,000	1	Node Classification
Questions	48,921	153,540	1	Node Classification

Table 6: The grid of hyperparameters employed during model selection for the graph transfer tasks (*Transfer*), graph property prediction tasks (*GPP*), Long Range Graph Benchmark (*LRGB*), and heterophilic benchmarks (*Hetero*).

Hyperparameters	Values			
	Transfer	***GPP***	***LRGB***	***Hetero***
Optimizer	Adam	Adam	AdamW	AdamW
Learning rate	0.001	0.003	0.001	0.001, 0.0005
Weight decay	0	10^{-6}	0	0
Dropout	0	0	0, 0.2, 0.5	0, 0.2, 0.5
N. recurrences	distance/2, distance	5, 10, 20	1,2,4,6,8,12,16	1,2,4,6,8,12,16
Embedding dim	64	30	60, 68, 74, 105, 117, 136	64, 128, 256, 512
N. Blocks	1,2	1, 2	1,2,3,4,5	from 1 to 12
ϵ	0.05, 0.1, 0.5, 1	0.001, 0.1, 0.5, 1	0.01, 0.02, 0.025, 0.05, 0.1	0.0001, 0.0005, 0.001, 0.005, 0.01, 0.05, 0.1
Use Dissipation			True, False	
Use External Force			True, False	
Use Adaptive Resistance			True, False	
$\mathbf{L}$			$\mathbf{D}-\mathbf{A}$, $\mathbf{I}-\mathbf{D}^{-1/2}\mathbf{A}\mathbf{D}^{-1/2}$, $\mathbf{I}-\mathbf{D}^{-1}\mathbf{A}$	

B Proofs of the Theoretical Results

In this section, we prove the theoretical results in Section 3.3.

B.1 Proof of Theorem 3.1

To prove Theorem 3.1, we first need this preliminary lemma:

Lemma B.1. *Let $\mathbf{X} \in \mathbb{R}^n$ be a feature vector for the nodes in graph $\mathcal{G}$. Then, it holds that*

$$\sum_{v \in V} \|\nabla \mathbf{x}_v(t)\|^2 = \sum_{v \in V} \sum_{u \in \mathcal{N}_v} (\mathbf{x}_v - \mathbf{x}_u)^2 = \frac{1}{2} \sum_{u,v \in V} \mathbf{A}_{vu} (\mathbf{x}_v - \mathbf{x}_u)^2 = \mathbf{X}^\top \mathbf{L} \mathbf{X} \tag{16}$$

The lemma involves only one feature per node, but it can easily be generalized to multiple features by considering norms and scalar products.

Proof of Lemma B.1. The first equivalence comes from the gradient definition in a graph (see [34]), while the second follows from expanding the sum of neighbors. We now show the last equivalence:

$$\begin{aligned}
\frac{1}{2}\sum_{u,v\in V}\mathbf{A}_{vu}(\mathbf{x}_v-\mathbf{x}_u)^2 &= \frac{1}{2}\sum_v\sum_u\mathbf{A}_{uv}(\mathbf{x}_v^2+\mathbf{x}_u^2-2\mathbf{x}_v\mathbf{x}_u)\\
&= \frac{1}{2}\sum_v\mathbf{x}_v^2\sum_u\mathbf{A}_{uv}+\sum_u\mathbf{x}_u^2\sum_v\mathbf{A}_{vu}-2\sum_{u,v}\mathbf{A}_{vu}\mathbf{x}_v\mathbf{x}_u\\
&= \frac{1}{2}\left(\sum_v\mathbf{x}_v^2\text{deg}(v)+\sum_u\mathbf{x}_u^2\text{deg}(u)-2\sum_{uv}\mathbf{A}_{uv}\mathbf{x}_u\mathbf{x}_v\right)\\
&= \frac{1}{2}\left(2\sum_v\mathbf{x}_v^2\mathbf{D}_{vv}-2\sum_{uv}\mathbf{A}_{uv}\mathbf{x}_u\mathbf{x}_v\right)\\
&= \sum_{v\in V}\mathbf{x}_v\left(\mathbf{x}_v\mathbf{D}_{vv}-\sum_u\mathbf{A}_{vu}\mathbf{x}_u\right)\\
&= \sum_{v\in V}\mathbf{x}_v\left(\mathbf{x}_v\mathbf{D}_{vv}\sum_u(\delta_{uv}\mathbf{x}_u-\mathbf{A}_{vu}\mathbf{x}_u)\right)\\
&= \sum_{v\in V}\mathbf{x}_v\sum_u(\mathbf{D}_{uu}\delta_{uv}-\mathbf{A}_{vu})\mathbf{x}_u\\
&= \sum_v\sum_u\mathbf{x}_v(\mathbf{D}_{uu}\delta_{uv}-\mathbf{A}_{uv})\mathbf{x}_u\\
&= \sum_{uv}\mathbf{x}_u\mathbf{L}\mathbf{x}_v=\mathbf{X}^\top\mathbf{L}\mathbf{X}
\end{aligned} \tag{17}$$

where δ_{uv} is 1 if $u=v$ and 0 otherwise. □

Proof of Theorem 3.1. We show the theorem for $d=1$ (one feature), since it involves the norms of the feature vector $\mathbf{X}(t)$. To improve clarity, here we consider the initial considtion to be $\mathbf{X}(0)=\bar{\mathbf{X}}=\bar{\mathbf{X}}$. The wave (4) has an explicit solution (see [34]) given by

$$\mathbf{X}(t)=\cos\left(t\sqrt{\mathbf{L}}\right)\bar{\mathbf{X}}, \tag{18}$$

where

$$\cos\left(t\sqrt{\mathbf{L}}\right)=I-\frac{t^2}{2}\mathbf{L}+\frac{t^4}{4!}\mathbf{L}^2+\ldots=\sum_{n=0}^{\infty}(-1)^n\frac{t^{2n}}{n!}\sqrt{\mathbf{L}}^{2n}. \tag{19}$$

The energy in (9) can be calculated as

$$\begin{aligned}
E(t) &= \frac{1}{2}\left(\sum_{v\in V}\|\nabla\mathbf{x}_v(t)\|^2+\left\|\frac{\partial\mathbf{X}(t)}{\partial t}\right\|^2\right)\\
&= \frac{1}{2}\left(\mathbf{X}(t)^\top\mathbf{L}\mathbf{X}(t)+\left(\frac{\partial(\cos\left(t\sqrt{\mathbf{L}}\right)\bar{\mathbf{X}})}{\partial t}\right)^2\right),
\end{aligned} \tag{20}$$

where we used the Lemma B.1for the first term and the explicit solution for the second. Using the explicit solution, the first term is equal to

$$\begin{aligned}
\mathbf{X}(t)^\top\mathbf{L}\mathbf{X}(t) &= \left(\cos\left(t\sqrt{\mathbf{L}}\right)\bar{\mathbf{X}}\right)^\top\mathbf{L}(\cos\left(t\sqrt{\mathbf{L}}\right)\bar{\mathbf{X}}\\
&= (\bar{\mathbf{X}})^\top\cos\left(t\sqrt{\mathbf{L}}\right)^\top\mathbf{L}\cos\left(t\sqrt{\mathbf{L}}\right)\bar{\mathbf{X}}\\
&= \left\|\sqrt{\mathbf{L}}\cos\left(t\sqrt{\mathbf{L}}\right)\bar{\mathbf{X}}\right\|^2\\
&= \left\|\cos\left(t\sqrt{\mathbf{L}}\right)\sqrt{\mathbf{L}}\bar{\mathbf{X}}\right\|^2,
\end{aligned} \tag{21}$$

where the last equality follows from the fact that $\cos\left(t\sqrt{\mathbf{L}}\right)$ and $\sqrt{\mathbf{L}}$ commute, which follows from the Taylor series expansion in (19). The second term can be calculated as

$$\frac{\partial}{\partial t}\left(\sum_{n=0}^{\infty}(-1)^n\frac{t^{2n}}{2n!}\sqrt{\mathbf{L}}^{2n}\right)\bar{\mathbf{X}} = \left(\sum_{n=1}^{\infty}(-1)^{n-1}\frac{t^{2n-1}}{(2n-1)!}\sqrt{\mathbf{L}}^{2n}\right)\bar{\mathbf{X}}. \tag{22}$$

which, using the Taylor series expansion of $\sin\left(t\sqrt{\mathbf{L}}\right)$, is equal to

$$\left\|\frac{\partial \mathbf{X}(t)}{\partial t}\right\|^2 = \left\|\sqrt{\mathbf{L}}\sin\left(t\sqrt{\mathbf{L}}\right)\bar{\mathbf{X}}\right\|^2 = \left\|\sin\left(t\sqrt{\mathbf{L}}\right)\sqrt{\mathbf{L}}\bar{\mathbf{X}}\right\|^2 \tag{23}$$

Finally, the sum of the two terms is equal to

$$\begin{aligned}
E(t) &= \frac{1}{2}\left(\left\|\cos\left(t\sqrt{\mathbf{L}}\right)\sqrt{\mathbf{L}}\bar{\mathbf{X}}\right\|^2 + \left\|\sin\left(t\sqrt{\mathbf{L}}\right)\sqrt{\mathbf{L}}\bar{\mathbf{X}}\right\|^2\right)\\
&= \frac{1}{2}\left((\bar{\mathbf{X}})^\top\sqrt{\mathbf{L}}^\top\cos\left(t\sqrt{\mathbf{L}}\right)^\top\cos\left(t\sqrt{\mathbf{L}}\right)\sqrt{\mathbf{L}}\bar{\mathbf{X}} + (\bar{\mathbf{X}})^\top\sqrt{\mathbf{L}}^\top\sin\left(t\sqrt{\mathbf{L}}\right)^\top\sin\left(t\sqrt{\mathbf{L}}\right)\sqrt{\mathbf{L}}\bar{\mathbf{X}}\right)\\
&= \frac{1}{2}\left((\bar{\mathbf{X}})^\top\sqrt{\mathbf{L}}\cos^2\left(t\sqrt{\mathbf{L}}\right)\sqrt{\mathbf{L}}\bar{\mathbf{X}} + (\bar{\mathbf{X}})^\top\sqrt{\mathbf{L}}\sin^2\left(t\sqrt{\mathbf{L}}\right)\sqrt{\mathbf{L}}\bar{\mathbf{X}}\right)\\
&= \frac{1}{2}\left((\bar{\mathbf{X}})^\top\sqrt{\mathbf{L}}\left(\cos^2\left(t\sqrt{\mathbf{L}}\right) + \sin^2\left(t\sqrt{\mathbf{L}}\right)\right)\sqrt{\mathbf{L}}\bar{\mathbf{X}}\right)\\
&= \frac{1}{2}\left((\bar{\mathbf{X}})^\top\sqrt{\mathbf{L}}\sqrt{\mathbf{L}}\bar{\mathbf{X}}\right) = \frac{1}{2}\left((\bar{\mathbf{X}})^\top\mathbf{L}\bar{\mathbf{X}}\right) = E(0),
\end{aligned} \tag{24}$$

Where the transpositions for $\sqrt{\mathbf{L}}$, $\sin$, and $\cos$ vanish as they are all symmetric matrices (since $\mathbf{L}$ is symmetric and positive definite, we can choose a symmetric square root). □

We now prove a general version of Theorem 3.1 with d features $\mathbf{X}(t) \in \mathbb{R}^{n\times d}$ and $\mathbf{W} = \mathbf{I}$.

Theorem B.1. *Let $\mathbf{X}(t) \in \mathbb{R}^{n\times d}$ be the node states at time t, obtained as the solution to the graph wave equation in Equation* (5)*, with initial condition $\mathbf{X}(0) = \bar{\mathbf{X}}$, null dissipative and external forcing terms, and $\mathbf{W} = \mathbf{I}$. Then, the energy $E(t)$, defined as*

$$E(t) = \sum_{v\in V}\frac{1}{2}\|\nabla\mathbf{x}_v(t)\|^2 + \frac{1}{2}\left\|\frac{\partial\mathbf{X}(t)}{\partial t}\right\|^2, \tag{25}$$

is conserved, that is, $E(t) = E(0)\ \forall t > 0$.

Proof. The proof is almost identical to the one from Theorem Theorem 3.1. Since features are not coupled, the solution to the equation is the same as Equation (10), and the same steps apply. Since we work with multiple features, scalar norms become vector norms, while the latter become matrix norms. □

B.2 Proof of Theorem 3.2

While the proof of Theorem 3.2 is a direct consequence of the explicit solution, we now prove a more general version of it for node states with d features and $\mathbf{W} = \mathbf{I}$.

Theorem B.2 (Sensitivity matrix, continuous case)**.** *Let $\mathbf{x}_v(t) \in \mathbb{R}^d$ be the state for node v at time t. Then, the sensitivity matrix $\frac{\partial\mathbf{x}_v(t)}{\partial\mathbf{x}_u(0)}$ between nodes u and v is*

$$\frac{\partial\mathbf{x}_v(t)}{\partial\mathbf{x}_u(0)} = \cos\left(t\sqrt{\mathbf{L}}\right)_{vu}\mathbf{I}. \tag{26}$$

Proof. Since $\mathbf{W} = \mathbf{I}$, the analytic solution to the SONAR wave equation in Equation (4) is the vector version of Equation (10)

$$\mathbf{X}(t) = \cos\left(t\sqrt{\mathbf{L}}\right)\bar{\mathbf{X}} = \cos\left(t\sqrt{\mathbf{L}}\right)\mathbf{X}(0) \tag{27}$$

Now, by differentiating with respect to $\mathbf{x}_u(0)$, we obtain

$$\frac{\partial \mathbf{x}_v(t)}{\partial \mathbf{x}_u(0)} = \cos\left(t\sqrt{\mathbf{L}}\right)_{vu} \mathbf{I}. \tag{28}$$

□

While Theorem B.1 and Theorem B.2 are not the most general statements with any possible feature coupling, we are the first to show proofs for the wave equation for graphs involving multidimensional features. Most of the works in the mathematical literature on the graph-based Laplacian and graph wave equation involve only the scalar case with single-valued functions [34, 53]

B.3 Proof of Theorem 3.3

Proof. We start by recalling the Sonar update with null dissipative and external forcing term

$$\begin{cases} \mathbf{X}^{\ell+1} = \mathbf{X}^{\ell} + h\mathbf{V}^{\ell+1}, \\ \mathbf{V}^{\ell+1} = \mathbf{V}^{\ell} - h\left(\mathbf{L}\mathbf{X}^{\ell}\mathbf{W}\right), \end{cases} \tag{29}$$

Substituting the second equation in the first one, we obtain

$$\begin{aligned} \mathbf{X}^{\ell+1} &= \mathbf{X}^{\ell} + h\mathbf{V}^{\ell} - h^2\mathbf{L}\mathbf{X}^{\ell}\mathbf{W} \\ &= \mathbf{X}^{\ell} + h\frac{\mathbf{X}^{\ell} - \mathbf{X}^{\ell-1}}{h} - h^2\mathbf{L}\mathbf{X}^{\ell}\mathbf{W} \\ &= 2\mathbf{X}^{\ell} - \mathbf{X}^{\ell-1} - h^2\mathbf{L}\mathbf{X}^{\ell}\mathbf{W} \end{aligned} \tag{30}$$

We now write the update for a single node v

$$\mathbf{x}_v^{\ell+1} = 2\mathbf{x}_v^{\ell} - \mathbf{x}_v^{\ell-1} - h^2 \sum_{u\in\mathcal{V}} \mathbf{L}_{vu}\mathbf{x}_u^{\ell}\mathbf{W} \tag{31}$$

Therefore, if we consider any node $u \in \mathcal{V}$, the one-step sensitivity matrix can be directly calculated by differentiating Equation 31 by $\mathbf{x}_u$. Since the dynamical system is causal, we have that $\frac{\partial \mathbf{x}_v^{\ell-1}}{\partial \mathbf{x}_u^{\ell}} = 0$ and, finally,

$$\frac{\partial \mathbf{x}_v^{\ell}}{\partial \mathbf{x}_u^{\ell-1}} = 2\mathbf{I}_{uv} - h^2\mathbf{L}_{uv}\mathbf{W}, \tag{32}$$

with $\mathbf{I}_{uv}$ denoting the (u, v)-th entry of the identity matrix. □

B.4 Proof of Theorem 3.4

Proof of Theorem 3.4. Let us consider one update of the wave equation solution from equation 7

$$\begin{aligned} \mathbf{X}^{\ell+1} &= \mathbf{X}^{\ell} + h\mathbf{V}^{\ell+1} \\ \mathbf{V}^{\ell+1} &= \mathbf{V}^{\ell} - hL\mathbf{X}^{\ell}\mathbf{W} - h\mathbf{k}(\mathbf{X}^{\ell}) \odot \mathbf{V}^{\ell} + h\mathbf{F}(\mathbf{X}^{\ell}) \end{aligned} \tag{33}$$

We will now show that

$$\left\| \frac{\partial \mathbf{x}_v^{\ell}}{\partial \mathbf{x}_u^{0}} \right\|_{L^1} \leq (wd)^{\ell} \left(\left((1 + h + h^2(N + k + 1))\mathbf{I} + h^2\mathbf{A}\right)^{\ell} \right)_{vu} \tag{34}$$

and

$$\left\| \frac{\partial \mathbf{v}_v^{\ell}}{\partial \mathbf{x}_u^{0}} \right\|_{L^1} \leq (wd)^{\ell} \left(\left((1 + h(N + k + 1))\mathbf{I} + h\mathbf{A}\right)^{\ell} \right)_{vu} \tag{35}$$

by induction, following [19].

Base case $\ell = 1$. Using the update equations, it is clear that

$$\left|\frac{\partial \mathbf{x}_v^{1,\alpha}}{\partial \mathbf{x}_u^{0,\beta}}\right| \leq \delta_{vu} + \delta_{vu} h \left|\frac{\partial \mathbf{v}_v^{1,\alpha}}{\partial \mathbf{x}_u^{0,\beta}}\right| \tag{36}$$

and

$$\left|\frac{\partial \mathbf{v}_v^{1,\alpha}}{\partial \mathbf{x}_u^{0,\beta}}\right| = \delta_{vu}\left(\left|\frac{\partial \mathbf{v}_v^{0,\alpha}}{\partial \mathbf{x}_u^{0,\beta}}\right| + hk\left|\frac{\partial \mathbf{v}_v^{0,\gamma}}{\partial \mathbf{x}_u^{0,\beta}}\right| + |h\mathbf{W}_F^{\alpha\beta}|\right) + h|\mathbf{L}_{vw}|\left|\frac{\partial \mathbf{x}_w^{0,\gamma}}{\partial \mathbf{x}_u^{0,\beta}}\right||\mathbf{W}^{\gamma\beta}|. \tag{37}$$

Since $\left|\frac{\partial \mathbf{v}_v^{0,\alpha}}{\partial \mathbf{x}_v^{0,\beta}}\right| = |\mathbf{W}_V^{\alpha\beta}| \leq w$, we have that

$$\left|\frac{\partial \mathbf{v}_v^{1,\alpha}}{\partial \mathbf{x}_u^{0,\beta}}\right| \leq \delta_{vu} w(1 + hk + h) + |\mathbf{L}_{vu}|wh \leq \delta_{vu} w\left(1 + h(N + k + 1)\right) + \mathbf{A}_{uv} wh \tag{38}$$

which, by summing over β and maximizing on α

$$\left\|\frac{\partial \mathbf{v}_v^1}{\partial \mathbf{x}_u^0}\right\|_{L^1} \leq (d)\left((1 + h(N + k + 1))\mathbf{I} + h\mathbf{A}\right)_{vu}, \tag{39}$$

and, by applying the same reasoning to equation 36

$$\left\|\frac{\partial \mathbf{x}_v^1}{\partial \mathbf{x}_u^0}\right\|_{L^1} \leq (wd)\left((1 + h + h^2(k + N + 1))\mathbf{I} + h^2\mathbf{A}\right)_{vu}. \tag{40}$$

Inductive step, $\ell \to \ell + 1$**.** We start by noticing that

$$\left|\frac{\partial \mathbf{x}_v^{\ell+1,\alpha}}{\partial \mathbf{x}_u^{0,\beta}}\right| \leq \delta_{vu}\left(\left|\frac{\partial \mathbf{x}_v^{\ell,\alpha}}{\partial \mathbf{x}_u^{0,\beta}}\right| + h\left|\frac{\partial \mathbf{v}_v^{\ell+1,\alpha}}{\partial \mathbf{x}_u^{0,\beta}}\right|\right), \tag{41}$$

which can be further decomposed as

$$\left|\frac{\partial \mathbf{x}_v^{\ell+1,\alpha}}{\partial \mathbf{x}_u^{0,\beta}}\right| \leq \left(\left|\frac{\partial \mathbf{x}_v^{\ell,\alpha}}{\partial \mathbf{x}_u^{0,\beta}}\right| + h\left|\frac{\partial \mathbf{v}_v^{\ell+1,\alpha}}{\partial \mathbf{x}_w^{\ell,\gamma}}\right|\left|\frac{\partial \mathbf{x}_w^{\ell,\gamma}}{\partial \mathbf{x}_u^{0,\beta}}\right| + h\left|\frac{\partial \mathbf{v}_v^{\ell+1,\alpha}}{\partial \mathbf{v}_w^{\ell,\gamma}}\right|\left|\frac{\partial \mathbf{v}_w^{\ell,\gamma}}{\partial \mathbf{x}_u^{0,\beta}}\right|\right). \tag{42}$$

It is easy to see that

$$\begin{aligned}\left|\frac{\partial \mathbf{v}_v^{\ell+1,\alpha}}{\partial \mathbf{x}_w^{\ell,\gamma}}\right| &\leq h|\mathbf{L}_{vw}|w + hw\delta_{vu} \leq \delta_{vw} hw(N + 1) + wh\mathbf{A}_{vw},\\ \left|\frac{\partial \mathbf{v}_v^{\ell+1,\alpha}}{\partial \mathbf{v}_w^{\ell,\gamma}}\right| &\leq \delta_{vw}(1 + hk).\end{aligned} \tag{43}$$

We now calculate

$$\begin{aligned}\left|\frac{\partial \mathbf{v}_w^{\ell+1,\alpha}}{\partial \mathbf{x}_u^{0,\beta}}\right| &\leq \delta_{wu}\left((1 + hk)\left|\frac{\partial \mathbf{v}_w^{\ell,\alpha}}{\partial \mathbf{x}_u^{0,\beta}}\right| + wh\left|\frac{\partial \mathbf{x}_w^{\ell,\alpha}}{\partial \mathbf{x}_u^{0,\beta}}\right|\right) + hw|\mathbf{L}_{wu}|\left|\frac{\partial \mathbf{x}_w^{\ell,\alpha}}{\partial \mathbf{x}_u^{0,\beta}}\right|\\ &\leq \delta_{wu}\left((1 + hk)\left\|\frac{\partial \mathbf{v}_w^{\ell}}{\partial \mathbf{x}_u^{0}}\right\|_{L^1} + wh(N + 1)\left\|\frac{\partial \mathbf{x}_w^{\ell}}{\partial \mathbf{x}_u^{0}}\right\|_{L^1}\right) + hw\mathbf{A}_{wu}\left\|\frac{\partial \mathbf{x}_w^{\ell}}{\partial \mathbf{x}_u^{0}}\right\|_{L^1}\end{aligned} \tag{44}$$

We now expand this last expression by inductive hypothesis and discard the terms with $O(h^2)$ as they become $O(h^3)$ in the next step. Summing over β and maximizing over α we get

$$\left|\frac{\partial \mathbf{v}_w^{\ell+1,\alpha}}{\partial \mathbf{x}_u^{0,\beta}}\right| \leq (wd)^{\ell+1}\left(\left((1 + h(N + k + 1))\mathbf{I} + h\mathbf{A}\right)^{\ell+1}\right)_{vu}. \tag{45}$$

which proves the inductive step for the sensitivity matrix on $\mathbf{V}$. We are now ready to prove the final part. Starting from equation 42, plugging in equation 43, we get

$$\begin{aligned}\left|\frac{\partial \mathbf{x}_v^{\ell+1,\alpha}}{\partial \mathbf{x}_u^{0,\beta}}\right| &\leq \left(\left\|\frac{\partial \mathbf{x}_v^{\ell}}{\partial \mathbf{x}_u^{0}}\right\|_{L^1} + h\left|\frac{\partial \mathbf{v}_v^{\ell+1,\alpha}}{\partial \mathbf{x}_w^{\ell,\gamma}}\right|\left\|\frac{\partial \mathbf{x}_w^{\ell}}{\partial \mathbf{x}_u^{0}}\right\|_{L^1} + h\left|\frac{\partial \mathbf{v}_v^{\ell+1,\alpha}}{\partial \mathbf{v}_w^{\ell,\gamma}}\right|\left\|\frac{\partial \mathbf{v}_w^{\ell}}{\partial \mathbf{x}_u^{0}}\right\|_{L^1}\right)\\ &\leq \left\|\frac{\partial \mathbf{x}_v^{\ell}}{\partial \mathbf{x}_u^{0}}\right\|_{L^1} + h(\delta_{vw} hw(N + 1) + wh\mathbf{A}_{vw})\left\|\frac{\partial \mathbf{x}_w^{\ell}}{\partial \mathbf{x}_u^{0}}\right\|_{L^1} + h(1 + hk)\delta_{vw}\left\|\frac{\partial \mathbf{v}_w^{\ell}}{\partial \mathbf{x}_u^{0}}\right\|_{L^1}\\ &\leq (wd)^{\ell}\left(\left((1 + h + h^2(N + k + 1))\mathbf{I} + h^2\mathbf{A}\right)^{\ell}\right)_{vu} +\\ &\quad + h(\delta_{vw} hw(N + 1) + wh\mathbf{A}_{vw})(wd)^{l}\left(\left((1 + h + h^2(N + k + 1))\mathbf{I} + h^2\mathbf{A}\right)^{\ell}\right)_{wu} +\\ &\quad + \delta_{vw} wh(1 + hk)(wd)^{\ell}\left(\left((1 + h(N + k + 1))\mathbf{I} + h\mathbf{A}\right)^{\ell}\right)_{wu}\end{aligned} \tag{46}$$

Summing over the last two terms and discarding the terms $O(h^3)$, we have

$$\left|\frac{\partial \mathbf{x}_v^{\ell+1,\alpha}}{\partial \mathbf{x}_u^{0,\beta}}\right| \leq (wd)^\ell \left(\left((1+h+h^2(N+k+1))\mathbf{I}+h^2\mathbf{A}\right)^\ell\right)_{vu} + \\ + (wd)^\ell wh((1+h(N+k+1))\delta_{vw}+h\mathbf{A}_{vw})\left(\left((1+h+h^2(N+k+1))\mathbf{I}+h^2\mathbf{A}\right)^\ell\right)_{wu} \tag{47}$$

Now we put δ_{vw} in front over the first term (and sum over w) to join the two terms together obtaining

$$\begin{aligned}
&\left|\frac{\partial \mathbf{x}_v^{\ell+1,\alpha}}{\partial \mathbf{x}_u^{0,\beta}}\right| \leq \delta_{vw}(wd)^\ell \left(\left((1+h+h^2(N+k+1))\mathbf{I}+h^2\mathbf{A}\right)^\ell\right)_{vw} + \\
&+ (wd)^\ell wh((1+h(N+k+1))\delta_{vw}+h\mathbf{A}_{vw})\left(\left((1+h+h^2(N+k+1))\mathbf{I}+h^2\mathbf{A}\right)^\ell\right)_{wu} \\
&= w^{\ell+1}d^\ell((1+h+h^2(N+k+1))\delta_{vw}+h^2\mathbf{A}_{vw})\left(\left((1+h+h^2(N+k+1))\mathbf{I}+h^2\mathbf{A}\right)^\ell\right)_{wu} \\
&= w^{\ell+1}d^\ell\left(\left((1+h^2(N+k+1))\mathbf{I}+h^2\mathbf{A}\right)^{\ell+1}\right)_{vu}
\end{aligned} \tag{48}$$

Summing over β gives the additional factor d, while maximizing over α gives us the thesis. □

C Additional Results And Comparisons

C.1 Extended Comparison

To further evaluate the performance of SONAR, we report a more complete comparison for the LRGB tasks in Table 7 and for the heterophilic tasks in Table 8. Specifically, in the LRGB setting, we include more multi-hop DGNs and ablate on the scores obtained with the original setting from [24] and the one proposed in [82]. The latter incorporates added residual connections and 3-layers MLP decoder. In the heterophilic setting, we include more MPNN-based models, graph transformers, and heterophily-designated GNNs. In both tables, we color the top three methods. Different from the main body of the paper, here we also include sub-variants of methods in the highlighted results, providing an additional perspective on the findings. Notably, our SONAR achieves state-of-the-art performance across all considered tasks.

C.2 Ablations

To better understand the contribution of each component in SONAR, we conduct a series of ablation studies.

Adaptive Resistance, Dissipation, and External Forces. We analyze the role of the dissipation mechanism, the external force term, and the adaptive edge resistance in shaping the model's dynamics and performance. Each of these components plays a crucial role in controlling information propagation over the graph. By systematically removing these elements, we assess their individual impact on long-range information flow and overall predictive performance.

Table 9 reports the mean and standard deviations on the test set for some tasks we analyzed in Section 4, i.e., graph transfer line-50, SSSP, Peptides-struct, and Roman-Empire. We report the results for each possible combination of adaptive resistance (i.e., adaptively re-computing the edge resistance at each step), dissipative, and external forcing components. We note that the importance of each component in SONAR varies depending on the task and the nature of the information it involves. In the graph transfer task, all components of SONAR are essential, particularly dissipation and external forcing as intermediate nodes contain random features that must be effectively filtered out. In the SSSP task, re-computing the resistances at each step leads to a performance drop, indicating that a constant propagation pattern is preferable. For `peptides-struct`, the external forcing term proves to be the most impactful, while dissipation offers little benefit. The best results on the `Roman-Empire` dataset are achieved using the purely conservative form of SONAR, highlighting the value of a non-dissipative signal propagation in that setting.

Lastly, to understand the importance of the energy preservation behavior of our SONAR, we compare its performance with that of a standard GCN, which can be considered as the most comparable baselines to our proposed SONAR. Both rely on the Laplacian operator and message-passing paradigm,

Table 7: Results for Peptides-func, Peptides-struct and PascalVOC-SP averaged over 3 training seeds. Baseline results are taken from [24, 46, 51, 82, 65, 21, 40, 52, 21]. Re-evaluated methods employ the 3-layer MLP readout proposed in [82]. Note that all MPNN-based methods include structural and positional encoding. The **first**, **second**, and **third** best scores are colored. ‡ means 3-layer MLP readout and residual connections are employed.

Model	Peptides-func AP ↑	Peptides-struct MAE ↓	Pascal VOC-SP F1 ↑
MPNNs			
GatedGCN	$58.64_{\pm 0.77}$	$0.3420_{\pm 0.0013}$	$0.2873_{\pm 0.0219}$
GCN	$59.30_{\pm 0.23}$	$0.3496_{\pm 0.0013}$	$0.1268_{\pm 0.0060}$
GCNII	$55.43_{\pm 0.78}$	$0.3471_{\pm 0.0010}$	$0.1698_{\pm 0.0080}$
GINE	$54.98_{\pm 0.79}$	$0.3547_{\pm 0.0045}$	$0.1265_{\pm 0.0076}$
Multi-hop GNNs			
DIGL+MPNN	$64.69_{\pm 0.19}$	$0.3173_{\pm 0.0007}$	$0.2824_{\pm 0.0039}$
DIGL+MPNN+LapPE	$68.30_{\pm 0.26}$	$0.2616_{\pm 0.0018}$	$0.2921_{\pm 0.0038}$
DRew-GCN	$69.96_{\pm 0.76}$	$0.2781_{\pm 0.0028}$	$0.1848_{\pm 0.0107}$
DRew-GCN+LapPE	**$71.50_{\pm 0.44}$**	$0.2536_{\pm 0.0015}$	$0.1851_{\pm 0.0092}$
DRew-GIN	$69.40_{\pm 0.74}$	$0.2799_{\pm 0.0016}$	$0.2719_{\pm 0.0043}$
DRew-GIN+LapPE	**$71.26_{\pm 0.45}$**	$0.2606_{\pm 0.0014}$	$0.2692_{\pm 0.0059}$
DRew-GatedGCN	$67.33_{\pm 0.94}$	$0.2699_{\pm 0.0018}$	$0.3214_{\pm 0.0021}$
DRew-GatedGCN+LapPE	$69.77_{\pm 0.26}$	$0.2539_{\pm 0.0007}$	$0.3314_{\pm 0.0024}$
GRED	$70.85_{\pm 0.27}$	$0.2503_{\pm 0.0019}$	–
GRED+LapPE	**$71.33_{\pm 0.11}$**	**$0.2455_{\pm 0.0013}$**	–
MixHop-GCN	$65.92_{\pm 0.36}$	$0.2921_{\pm 0.0023}$	$0.2506_{\pm 0.0133}$
MixHop-GCN+LapPE	$68.43_{\pm 0.49}$	$0.2614_{\pm 0.0023}$	$0.2218_{\pm 0.0174}$
Transformers			
GraphGPS+LapPE	$65.35_{\pm 0.41}$	$0.2500_{\pm 0.0005}$	$0.3748_{\pm 0.0109}$
Graph ViT	$69.42_{\pm 0.75}$	**$0.2449_{\pm 0.0016}$**	–
GRIT	$69.88_{\pm 0.82}$	**$0.2460_{\pm 0.0012}$**	–
SAN+LapPE	$63.84_{\pm 1.21}$	$0.2683_{\pm 0.0043}$	$0.3230_{\pm 0.0039}$
Transformer+LapPE	$63.26_{\pm 1.26}$	$0.2529_{\pm 0.0016}$	$0.2694_{\pm 0.0098}$
Modified and Re-evaluated‡			
GCN	$68.60_{\pm 0.50}$	**$0.2460_{\pm 0.0007}$**	$0.2078_{\pm 0.0031}$
GINE	$66.21_{\pm 0.67}$	$0.2473_{\pm 0.0017}$	$0.2718_{\pm 0.0054}$
GatedGCN	$67.65_{\pm 0.47}$	$0.2477_{\pm 0.0009}$	$0.3880_{\pm 0.0040}$
DRew-GCN+LapPE	$69.45_{\pm 0.21}$	$0.2517_{\pm 0.0011}$	–
GraphGPS+LapPE	$65.34_{\pm 0.91}$	$0.2509_{\pm 0.0014}$	**$0.4440_{\pm 0.0064}$**
DE-GNNs			
GRAND	$57.89_{\pm 0.62}$	$0.3418_{\pm 0.0015}$	$0.1918_{\pm 0.0097}$
GraphCON	$60.22_{\pm 0.68}$	$0.2778_{\pm 0.0018}$	$0.2108_{\pm 0.0091}$
A-DGN	$59.75_{\pm 0.44}$	$0.2874_{\pm 0.0021}$	$0.2349_{\pm 0.0054}$
SWAN	$67.51_{\pm 0.39}$	$0.2485_{\pm 0.0009}$	$0.3192_{\pm 0.0250}$
PH-DGN‡	$70.12_{\pm 0.45}$	$0.2465_{\pm 0.0020}$	–
Ours			
SONAR	$68.42_{\pm 0.11}$	$0.2525_{\pm 0.0038}$	**$0.4058_{\pm 0.0039}$**
SONAR+LapPE	$70.47_{\pm 0.41}$	$0.2486_{\pm 0.0006}$	**$0.4082_{\pm 0.0037}$**

Table 8: Mean test set score and std averaged over 4 random weight initializations on heterophilic datasets. The higher, the better. **First**, **second**, and **third** best results for each task are color-coded.

Model	Roman-empire Acc ↑	Amazon-ratings Acc ↑	Minesweeper AUC ↑	Tolokers AUC ↑	Questions AUC ↑
[64]					
MLP-2	$66.04_{\pm 0.71}$	$49.55_{\pm 0.81}$	$50.92_{\pm 1.25}$	$74.58_{\pm 0.75}$	$69.97_{\pm 1.16}$
SGC-1	$44.60_{\pm 0.52}$	$40.69_{\pm 0.42}$	$82.04_{\pm 0.77}$	$73.80_{\pm 1.35}$	$71.06_{\pm 0.92}$
MLP-1	$64.12_{\pm 0.61}$	$38.60_{\pm 0.41}$	$50.59_{\pm 0.83}$	$71.89_{\pm 0.82}$	$70.33_{\pm 0.96}$
Graph-agnostic					
ResNet	$65.88_{\pm 0.38}$	$45.90_{\pm 0.52}$	$50.89_{\pm 1.39}$	$72.95_{\pm 1.06}$	$70.34_{\pm 0.76}$
ResNet+SGC	$73.90_{\pm 0.51}$	$50.66_{\pm 0.48}$	$70.88_{\pm 0.90}$	$80.70_{\pm 0.97}$	$75.81_{\pm 0.96}$
ResNet+adj	$52.25_{\pm 0.40}$	$51.83_{\pm 0.57}$	$50.42_{\pm 0.83}$	$78.78_{\pm 1.11}$	$75.77_{\pm 1.24}$
MPNNs					
GAT	$80.87_{\pm 0.30}$	$49.09_{\pm 0.63}$	$92.01_{\pm 0.68}$	$83.70_{\pm 0.47}$	$77.43_{\pm 1.20}$
GAT-sep	**88.75**$_{\pm 0.41}$	$52.70_{\pm 0.62}$	$93.91_{\pm 0.35}$	$83.78_{\pm 0.43}$	$76.79_{\pm 0.71}$
GAT (LapPE)	$84.80_{\pm 0.46}$	$44.90_{\pm 0.73}$	$93.50_{\pm 0.54}$	**84.99**$_{\pm 0.54}$	$76.55_{\pm 0.84}$
GAT (RWSE)	$86.62_{\pm 0.53}$	$48.58_{\pm 0.41}$	$92.53_{\pm 0.65}$	**85.02**$_{\pm 0.67}$	$77.83_{\pm 1.22}$
GAT (DEG)	$85.51_{\pm 0.56}$	$51.65_{\pm 0.60}$	$93.04_{\pm 0.62}$	$84.22_{\pm 0.81}$	$77.10_{\pm 1.23}$
Gated-GCN	$74.46_{\pm 0.54}$	$43.00_{\pm 0.32}$	$87.54_{\pm 1.22}$	$77.31_{\pm 1.14}$	$76.61_{\pm 1.13}$
GCN	$73.69_{\pm 0.74}$	$48.70_{\pm 0.63}$	$89.75_{\pm 0.52}$	$83.64_{\pm 0.67}$	$76.09_{\pm 1.27}$
GCN (LapPE)	$83.37_{\pm 0.55}$	$44.35_{\pm 0.36}$	**94.26**$_{\pm 0.49}$	$84.95_{\pm 0.78}$	$77.79_{\pm 1.34}$
GCN (RWSE)	$84.84_{\pm 0.55}$	$46.40_{\pm 0.55}$	$93.84_{\pm 0.48}$	**85.11**$_{\pm 0.77}$	$77.81_{\pm 1.40}$
GCN (DEG)	$84.21_{\pm 0.47}$	$50.01_{\pm 0.69}$	**94.14**$_{\pm 0.50}$	$82.51_{\pm 0.83}$	$76.96_{\pm 1.21}$
SAGE	$85.74_{\pm 0.67}$	**53.63**$_{\pm 0.39}$	$93.51_{\pm 0.57}$	$82.43_{\pm 0.44}$	$76.44_{\pm 0.62}$
Graph Transformers					
Exphormer	**89.03**$_{\pm 0.37}$	**53.51**$_{\pm 0.46}$	$90.74_{\pm 0.53}$	$83.77_{\pm 0.78}$	$73.94_{\pm 1.06}$
NAGphormer	$74.34_{\pm 0.77}$	$51.26_{\pm 0.72}$	$84.19_{\pm 0.66}$	$78.32_{\pm 0.95}$	$68.17_{\pm 1.53}$
GOAT	$71.59_{\pm 1.25}$	$44.61_{\pm 0.50}$	$81.09_{\pm 1.02}$	$83.11_{\pm 1.04}$	$75.76_{\pm 1.66}$
GPS	$82.00_{\pm 0.61}$	**53.10**$_{\pm 0.42}$	$90.63_{\pm 0.67}$	$83.71_{\pm 0.48}$	$71.73_{\pm 1.47}$
$\text{GPS}_{\text{GCN+Performer}}$ (LapPE)	$83.96_{\pm 0.53}$	$48.20_{\pm 0.67}$	$93.85_{\pm 0.41}$	$84.72_{\pm 0.77}$	$77.85_{\pm 1.25}$
$\text{GPS}_{\text{GCN+Performer}}$ (RWSE)	$84.72_{\pm 0.65}$	$48.08_{\pm 0.85}$	$92.88_{\pm 0.50}$	$84.81_{\pm 0.86}$	$76.45_{\pm 1.51}$
$\text{GPS}_{\text{GCN+Performer}}$ (DEG)	$83.38_{\pm 0.68}$	$48.93_{\pm 0.47}$	$93.60_{\pm 0.47}$	$80.49_{\pm 0.97}$	$74.24_{\pm 1.18}$
$\text{GPS}_{\text{GAT+Performer}}$ (LapPE)	$85.93_{\pm 0.52}$	$48.86_{\pm 0.38}$	$92.62_{\pm 0.79}$	$84.62_{\pm 0.54}$	$76.71_{\pm 0.98}$
$\text{GPS}_{\text{GAT+Performer}}$ (RWSE)	$87.04_{\pm 0.58}$	$49.92_{\pm 0.68}$	$91.08_{\pm 0.58}$	$84.38_{\pm 0.91}$	$77.14_{\pm 1.49}$
$\text{GPS}_{\text{GAT+Performer}}$ (DEG)	$85.54_{\pm 0.58}$	$51.03_{\pm 0.60}$	$91.52_{\pm 0.46}$	$82.45_{\pm 0.89}$	$76.51_{\pm 1.19}$
$\text{GPS}_{\text{GCN+Transformer}}$ (LapPE)	OOM	OOM	$91.82_{\pm 0.41}$	$83.51_{\pm 0.93}$	OOM
$\text{GPS}_{\text{GCN+Transformer}}$ (RWSE)	OOM	OOM	$91.17_{\pm 0.51}$	$83.53_{\pm 1.06}$	OOM
$\text{GPS}_{\text{GCN+Transformer}}$ (DEG)	OOM	OOM	$91.76_{\pm 0.61}$	$80.82_{\pm 0.95}$	OOM
$\text{GPS}_{\text{GAT+Transformer}}$ (LapPE)	OOM	OOM	$92.29_{\pm 0.61}$	$84.70_{\pm 0.56}$	OOM
$\text{GPS}_{\text{GAT+Transformer}}$ (RWSE)	OOM	OOM	$90.82_{\pm 0.56}$	$84.01_{\pm 0.96}$	OOM
$\text{GPS}_{\text{GAT+Transformer}}$ (DEG)	OOM	OOM	$91.58_{\pm 0.56}$	$81.89_{\pm 0.85}$	OOM
GT	$86.51_{\pm 0.73}$	$51.17_{\pm 0.66}$	$91.85_{\pm 0.76}$	$83.23_{\pm 0.64}$	**77.95**$_{\pm 0.68}$
GT-sep	$87.32_{\pm 0.39}$	$52.18_{\pm 0.80}$	$92.29_{\pm 0.47}$	$82.52_{\pm 0.92}$	**78.05**$_{\pm 0.93}$
Heterophily-Designated GNNs					
CPGNN	$63.96_{\pm 0.62}$	$39.79_{\pm 0.77}$	$52.03_{\pm 5.46}$	$73.36_{\pm 1.01}$	$65.96_{\pm 1.95}$
FAGCN	$65.22_{\pm 0.56}$	$44.12_{\pm 0.30}$	$88.17_{\pm 0.73}$	$77.75_{\pm 1.05}$	$77.24_{\pm 1.26}$
FSGNN	$79.92_{\pm 0.56}$	$52.74_{\pm 0.83}$	$90.08_{\pm 0.70}$	$82.76_{\pm 0.61}$	**78.86**$_{\pm 0.92}$
GBK-GNN	$74.57_{\pm 0.47}$	$45.98_{\pm 0.71}$	$90.85_{\pm 0.58}$	$81.01_{\pm 0.67}$	$74.47_{\pm 0.86}$
GloGNN	$59.63_{\pm 0.69}$	$36.89_{\pm 0.14}$	$51.08_{\pm 1.23}$	$73.39_{\pm 1.17}$	$65.74_{\pm 1.19}$
GPR-GNN	$64.85_{\pm 0.27}$	$44.88_{\pm 0.34}$	$86.24_{\pm 0.61}$	$72.94_{\pm 0.97}$	$55.48_{\pm 0.91}$
H2GCN	$60.11_{\pm 0.52}$	$36.47_{\pm 0.23}$	$89.71_{\pm 0.31}$	$73.35_{\pm 1.01}$	$63.59_{\pm 1.46}$
JacobiConv	$71.14_{\pm 0.42}$	$43.55_{\pm 0.48}$	$89.66_{\pm 0.40}$	$68.66_{\pm 0.65}$	$73.88_{\pm 1.16}$
Our					
SONAR	**89.82**$_{\pm 0.57}$	$52.22_{\pm 0.14}$	**96.29**$_{\pm 0.73}$	$83.57_{\pm 1.44}$	$74.96_{\pm 1.10}$

Table 9: Mean test set results with standard deviations for different combinations of SONAR components. The last line presents the results from a standard GCN for the comparison with a non-conservative method. **First**, **second**, and **third** best results for each task are color-coded.

Adaptive Resistace	Dissipation	External Forcing	Line-50 $\log_{10}$(MSE) ↓	SSSP $\log_{10}$MSE ↓	Peptides-struct MAE ↓	Roman-Empire Acc ↑
✓	✓	✓	**-6.4069**$_{\pm 0.4653}$	-3.0213$_{\pm 0.2431}$	0.2611$_{\pm 0.0075}$	88.24$_{\pm 0.24}$
✓	✓	–	-5.7542$_{\pm 0.6264}$	-3.8182$_{\pm 0.2239}$	0.2592$_{\pm 0.0168}$	88.61$_{\pm 1.11}$
✓	–	✓	**-6.2545**$_{\pm 0.3354}$	-2.7857$_{\pm 0.1731}$	**0.2506**$_{\pm 0.0010}$	**89.27**$_{\pm 0.77}$
✓	–	–	-5.3827$_{\pm 0.4078}$	-2.8108$_{\pm 0.2010}$	0.2560$_{\pm 0.0098}$	**89.81**$_{\pm 0.57}$
–	✓	✓	**-6.3598**$_{\pm 0.5403}$	**-6.7515**$_{\pm 0.0589}$	0.2631$_{\pm 0.0052}$	88.95$_{\pm 0.57}$
–	✓	–	-5.9058$_{\pm 0.5576}$	**-6.5939**$_{\pm 0.2925}$	0.2508$_{\pm 0.0036}$	89.12$_{\pm 0.82}$
–	–	✓	-4.9749$_{\pm 0.2777}$	**-6.5241**$_{\pm 0.5738}$	**0.2486**$_{\pm 0.0006}$	89.22$_{\pm 0.41}$
–	–	–	-5.4487$_{\pm 0.7370}$	-6.3226$_{\pm 0.1126}$	**0.2503**$_{\pm 0.0006}$	**89.42**$_{\pm 0.67}$
GCN results for comparison			-3.5032$_{\pm 0.0001}$	0.9499$_{\pm 0.0001}$	0.3496$_{\pm 0.0013}$	73.69$_{\pm 0.74}$

Table 10: Mean train and test errors of identical SONAR models with different step sizes h on the Ring-10 task from Section 4.1.

step size h	mean train loss	mean test loss
0.05	0.0020273	0.0019732
0.10	0.0019947	0.0019512
0.50	0.0039039	0.0039458
1.00	0.0085834	0.0086960

but GCN lacks energy preservation guarantees for long-range information propagation, adaptive resistance, and external forces. We note that GCN fails in solving these tasks since it performs a dissipative signal propagation. As a result, information about distant nodes becomes increasingly indistinguishable and ultimately lost. In contrast, our SONAR successfully solves these tasks because it performs a non-dissipative propagation. This is enabled by explicitly preserving the energy of the system (Equation (9)) in its design, with the result of preserving signals during propagation (as theoretically discussed in Section 3).

Overall, these results highlight SONAR's ability to balance conservative and non-conservative behaviors, enhancing its ability to learn more complex and task-specific dynamics. We believe that the modular design of SONAR, with components that can be selectively activated, provides high flexibility and allows SONAR to adapt to a wide range of scenarios while maintaining computational efficiency, without relying on global attention mechanisms or graph rewiring.

This analysis also suggests a practical guideline: for propagation-heavy tasks, forcing (and often dissipation) is beneficial; dissipation is particularly useful under high noise (e.g., graph transfer tasks); and adaptive resistance tends to help particularly with heterophilic tasks. These trends narrow the hyperparameter search space, though a small hyperparameter search is still necessary for optimal performance.

The Effect of the Step-Size h. Since the step size controls the numerical accuracy of the wave equation, its careful selection is essential for preserving SONAR's properties and performance. As with classical numerical solvers for physical equations, a high number of iterations requires a smaller step size, and vice versa. In practice, we observed that small variations in the step size have little impact on performance, and exploring different orders of magnitude is sufficient to identify near-optimal values. For a practical example, we consider the ring-10 task described in Section 4.1 and train an identical configuration of SONAR with 4 different step sizes. The results, reported in Table 10, indicate that close step sizes produce comparable performance, with noticeable differences arising only for large changes. This demonstrates that SONAR's behavior is robust to small changes in the step size.

Runtimes. Additionally, we report runtime analyses to evaluate the computational efficiency of SONAR with respect to state-of-the-art methods in Table 11. Specifically, we report the training and inference times in milliseconds, as well as the memory usage obtained on the Roman-Empire dataset, fixing the model trainable parameters to 100k. As can be seen from the results in the Table, our

SONAR maintains a similar runtime and memory consumption to GCN, which has linear complexity with respect to the graph size. All runtimes are measured on an NVIDIA H100 GPU.

Table 11: Training and inference time (in milliseconds) and memory usage on the Roman-Empire dataset measured on a NVIDIA H100 GPU. All models have approximately 100k trainable parameters; GPS uses 2 attention heads.

		Depth			
Method	**Metrics**	**4**	**8**	**16**	**32**
GCN	Training (ms)	$3.32_{\pm 0.07}$	$5.08_{\pm 0.85}$	$7.99_{\pm 0.3}$	$13.04_{\pm 0.12}$
	Inference (ms)	$1.98_{\pm 0.02}$	$3.24_{\pm 0.06}$	$5.0_{\pm 0.07}$	$8.05_{\pm 0.04}$
	Training Mem (GB)	0.25	0.25	0.28	0.34
	Inference Mem (GB)	0.21	0.18	0.16	0.14
GPS	Training (ms)	$101.21_{\pm 0.25}$	$321.33_{\pm 1.27}$	$642.53_{\pm 0.54}$	OOM
	Inference (ms)	$88.51_{\pm 0.14}$	$157.31_{\pm 0.22}$	$287.27_{\pm 0.15}$	OOM
	Training Mem (GB)	0.35	43.59	75.13	OOM
	Inference Mem (GB)	15.79	15.78	15.78	OOM
SONAR (1 block)	Training (ms)	$10.11_{\pm 0.97}$	$18.01_{\pm 1.11}$	$32.62_{\pm 0.12}$	$63.18_{\pm 0.82}$
	Inference (ms)	$3.78_{\pm 0.04}$	$6.59_{\pm 0.02}$	$12.23_{\pm 0.03}$	$23.45_{\pm 0.09}$
	Training Mem (GB)	0.71	1.24	2.29	4.41
	Inference Mem (GB)	0.27	0.28	0.28	0.28
SONAR (2 blocks)	Training (ms)	$9.63_{\pm 0.18}$	$16.21_{\pm 0.1}$	$29.62_{\pm 0.09}$	$56.56_{\pm 0.47}$
	Inference (ms)	$4.03_{\pm 1.14}$	$5.87_{\pm 0.05}$	$10.47_{\pm 0.02}$	$19.74_{\pm 0.07}$
	Training Mem (GB)	0.57	0.97	1.77	3.37
	Inference Mem (GB)	0.23	0.23	0.23	0.23

D Limitations

This paper contributes to the field of machine learning by advancing (differential equation-inspired) graph neural networks, with a focus on enhancing long-range information propagation. Specifically, we introduce a novel methodology that enables provable long-range propagation on graphs, grounded in a physically interpretable model based on wave dynamics and their underlying properties.

While we believe our work offers a meaningful contribution, it is important to clarify that SONAR is designed to address the long-range propagation problem in GNNs through the lens of DE-GNNs. Therefore, our model prioritizes on problems that require effective modeling of long-range interaction while maintaining low computational overhead. However, if the goal is to maximize downstream performance regardless of computational complexity, alternative approaches such as multi-hop GNNs or graph transformers may also be appropriate.

A second limitation arises from SONAR's formulation as a discrete approximation of a continuous dynamical system. Its behavior depends on the discretization scheme, making the choice of the step size h crucial. As shown in Theorem 3.4, the sensitivity bound can grow exponentially with the number of steps, potentially leading to exploding gradients if h is not appropriately tuned. We emphasize, however, that this issue can be effectively mitigated through careful step size selection and was never encountered in our experiments.